J. Mol. Model. **1998**, *4*, 12 – 32

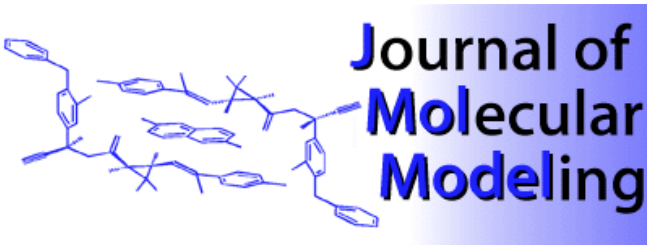

FULL PAPER

Nonlinear Charge Carriers in Polyacetylene

Wolfgang Förner[1] and Wolfram Utz[2]

[1] Box 2016, Chemistry Department, King Fahd University of Petroleum and Minerals, Dhahran 31261, Saudi Arabia.
E-mail: forner@dpc.kfupm.edu.sa

[2] Chair for Theoretical Chemistry, Friedrich-Alexander University, Egerlandstrasse 3, D-91058 Erlangen, Germany.
E-mail: utz@pctc.chemie.uni-erlangen.de

Submitted: 11 August 1997 / Accepted:9 December 1997 / Published: 9 January 1998

Abstract Conjugated organic polymers are intrinsically semiconductors but become conducting upon doping and photoconducting after optical excitation. In the low doping regime they show usually conduction without an associated spin transport. Thus as charge carriers in this regime nonlinear quasiparticles are assumed, such as charged solitons in materials with a degenerate ground state like e.g. *trans*-polyacetylene or pernigraniline. In the case of materials with a non-degenerate ground state the situation is often less clear but it is assumed that charged polarons or bipolarons are the charge carriers in them.

We present a theoretical model for the description of the dynamics of such quasiparticles which yields also information on their mobility, their nature and stability, as well as their spectral properties. The model is based on a π-electron Hamiltonian including electron-electron interactions. On the basis of the prototype material polyacetylene it is demonstrated how such a model can be parametrized with the help of correlated *ab initio* or density functional calculations and applied. We discuss in some detail the dynamics of the pristine material, as well as of doped and of electronically excited polyene chains. With the help of these dynamics a scenario for the conduction mechanism assumed for polyacetylene is given. Further we calculate optical spectra from the dynamics for charged solitons and for excited chains which are in fair agreement with experiments. The thermal mobility of neutral solitons is also studied.

Further we show how the model can be extended for applications to polymers different from polyacetylene. Such modifications could yield informations about the nature of nonlinear quasiparticles involved in the process of charge transport in cases where the question is not completely solved. This is the case in *cis*-polyacetylene where recent literature suggests that bipolarons should be instable. However, we could show that both charged polarons and bipolarons are stable in the material with bipolarons favored over charged polarons.

Due to the fact that the model can be extended to other polymers, also to chemical stuctures not yet synthesized, it could gain also predictive power after further development.

Keywords Conducting polymers, Nonlinear dynamics, Solitons, Polarons, Electronic spectra

Correspondence to: W. Förner

Introduction

Conjugated organic polymers nowadays play an important role as Synthetic Metals, because, though intrinsically semiconductors, they become conducting upon doping or optical excitation with conductivities even higher than that of metallic copper for heavily doped samples (see Ref. [1a-d] for a moderately recent review in Rev. Mod. Phys. where also the original literature is cited). It is in this field where concepts and *ansatz* states as introduced in Davydov soliton theory and outlined in our previous papers in this Journal [1e-g] can be applied with slight modifications to study, for example, the importance of lattice quantization. The interest in these materials as conductors originates from several facts. First of all they are cheaper than for example copper, secondly they can be synthesized in any desired amount and thirdly they are easily processible. From the theoretical side the unusual conduction properties especially of the lightly doped and photoconducting samples are most interesting, because these materials can transport charge without the transport of spin, i.e. the charge carriers cannot be simple electrons as in conventional metals. For theoreticians the most interesting synthetic metal naturally is polyacetylene because of the simplicity of its unit cell, while from the practical point of view materials like polyparaphenylene, polypyrrole or the different oxidation states of polyaniline are more interesting, because in contrast to polyacetylene they are stable against oxidation in air. We want to emphasize, that although we concentrated in our previous work as well as in this paper on polyacetylene, our models can be applied also to synthetic metals with larger unit cells, because we use the very simple semiempirical Pariser-Parr-Pople Hamiltonian for the description of the π-electrons of the polymers which play the major role in the conduction mechanisms. Thus in this work we want to demonstrate that our model is able to explain several properties of the charge carriers in polyacetylene and only in the Conclusion we want to describe shortly its application to polymers with larger unit cells. Applications to polyparaphenylene are currently planned at the Chemistry Department. The experimental fact that polyacetylene has a single EPR (Electronic Paramagnetic Resonance) line which exhibits motional line narrowing basically lead Su, Schrieffer and Heeger [1] already in the late 70-s to the idea that the charge carriers in these materials could be nonlinear quasiparticles, in case of *trans*-polyacetylene charged solitons. However, the simple model used by them was not sufficient.

Since the introduction of the soliton model and the Su-Schrieffer-Heeger (SSH) Hamiltonian [1] (for a recent comprehensive review see the article of Heeger, Kivelson, Schrieffer, and Su [1]) for the explanation of various properties of *trans*-polyacetylene (t-PA), it has been shown that it is necessary to go beyond the simple Hückel type SSH model. A Hückel type model for example, cannot explain the spin densities in t-PA measured with the electron-nuclear double resonance (ENDOR) method [2]. Also for the explanation of ^{13}C-NMR line shapes the inclusion of explicit electron-electron interactions into the model turned out to be essential [3]. The observed photo-induced low energy absorption was assigned to excitations from photo-generated charged soliton pairs which would absorb midgap in the SSH model [4]. The origin of the photo-induced high energy absorption, however, is still not sufficiently clear. Bishop *et al.* [5] assign it to a breather excitation left between a separating pair of charged solitons. Wang and Martino [6] found an oscillating charged soliton-antisoliton pair with a breather vibration of the chain between them to be responsible for this absorption, while Su [7a] and Kivelson *et al.* [7b] suggest a neutral (triplet) soliton pair as its origin. Therefore, it seems to be established that the inclusion of electron-electron interactions at least on the Pariser-Parr-Pople (PPP) level in mean field form is necessary to obtain a reasonable model of the dynamics of t-PA chains. Nowadays (see discussion and references in [8]) it is established that neutral solitons are indeed responsible for the high energy absorption. However, for the purpose of describing just the evolution of the chain geometry and the corresponding α-spin densities in time it seems to be sufficient to use the SSH model Hamiltonian. For this purpose a reduced value of the dimerization parameter (see Section II) u_0 has to be used, to account for the shrinking of the neutral soliton width upon inclusion of electron-electron interactions.

The computation of the gradient of the electronic energy with respect to the geometrical degrees of freedom can be done in a time consuming way by a small shift of the coordinate of each CH unit [9-12], however, the use of exact analytical gradients is more efficient [13]. In t-PA the soliton movement is restricted to less than 50 CC bonds [2] probably due to impurities, crosslinks, and *cis*-PA segments [14] or interchain interactions. Thus an open chain seems to be a more realistic model than a cyclic one. Wang and Martino [6] used an extended Hubbard model with first neighbour electron-electron interactions. This seems to be consistent with the first neighbour truncation of the resonance integrals. However, the resonance integrals decay very rapidly after the first neighbour term, while the two-electron integrals do not [15]. In our simulations using the full PPP Hamiltonian and the unrestricted Hartree-Fock (UHF) method we found that electron-electron interactions have a considerable influence on soliton properties [15]. Its kinetic mass for example, is roughly doubled compared to that in the SSH model [1] and its half width reduced in agreement with MNDO (modified neglect of differential overlap) calculations [16]. The MNDO method treats all valence electrons explicitely and not only the π-electrons as PPP does. However, in [16] restricted open shell HF (ROHF) was applied instead of a different orbitals for different spins (DODS) method like UHF or annihilated UHF (AUHF), which are more appropriate for open shell systems like neutral solitons in $(CH)_{2n+1}$ (polymethine) chains.

In a previous work we have studied the influence of isoelectronic substitutions of CH by N, NH^+, and O^+ within the SSH framework [10]. We found that a soliton is able to pass a nitrogen atom but not the oxygen. In another paper [17] site and bond impurities have been studied applying also the SSH theory. It was found by Phillpot *et al.* [17] that the soliton moves unperturbed in a rather broad range of the impurity strength. Since the soliton properties change con-

siderably upon inclusion of electron-electron interactions [15] it is important to study the effects of site and bond impurities also within the PPP model. This was done in our previous work [18] and we found that in the PPP model free soliton movement is possible within a much smaller range around the parameter values appropriate for carbon than in SSH models [10,17]. Similar conclusions were obtained from a model where the spin contaminations inherent in the UHF *ansatz* are avoided [19]. In a more recent work we attempted to reparametrize the PPP Hamiltonian for polyenes and found, that the electron-phonon interaction parameter has to be much smaller than that in the SSH Hamiltonian [20]. The results found in this study confirmed the assignment of the photoinduced low energy absorption to charged solitons and of the high energy absorption to neutral solitons.

Since in all our studies using the PPP Hamiltonian we found a rather small soliton half width of about 2-3 lattice sites the question of the influence of quantum effects on soliton dynamics in the lattice arises (see also the review by Heeger *et al.* [1]). In an early work, Nakahara and Maki [21] discussed quantum effects on the solitons on the basis of the continuum version of the SSH Hamiltonian. The discrete SSH-Hamiltonian was applied by Rukh *et al.* [22] who used an *ansatz* which is a product of one-electron states and displaced oscillator states for the lattice. Thus their *ansatz* is similar to the semiclassical $|D_2>$ *ansatz* state introduced by Davydov [23] for the treatment of protein solitons, where coupled high frequency oscillators interact with acoustical phonons in the lattice. Rukh *et al.* [22] found that quantum effects destroy the solitons when their size is small. Since in the PPP case the soliton size is rather small, one had to investigate quantum effects further. Going beyond the *ansatz* of Rukh *et al.* we used an *ansatz* derived from Davydov's more sophisticated $|D_1>$ state [24] which is a better approximation to the true quantum states of the Davydov Hamiltonian. However, in our case the state contains more than one quantum (electron) in contrast to Davydov's considerations. We derived the equations of motion from this *ansatz* for the SSH Hamiltonian [25]. Further we derived also the equations for some approximations to it, together with possibilities for the consideration of temperature effects. These include an intermediate one where the coherent state amplitudes for the lattice phonons depend only on the lattice site and the wavenumber of the phonons and a most simple one where electronic and lattice wave functions are separated, $|\Phi_2>$, corresponding to Davydov's $|D_2>$ *ansatz* in proteins (extensive discussions of Davydov's model and *ansätze*, as well as numerical applications can be found in refs. [26-34]). On the numerical side we restricted ourselves to applications of the equations of motion for the $|\Phi_2>$ *ansatz* state, where the product of one electron states is simply multiplied with a coherent state for the lattice phonons. However, the electrons were not assumed to follow the lattice dynamics instantaneously, as it is the case in the completely adiabatic model. This *ansatz* state is of interest, because Rukh *et al.* [22] used a similar model containing a product of electronic states with coherent phonon states, but treated only the electron occupying the soliton level explicitely. Since small soliton sizes can be easily obtained in the SSH Hamiltonian by using a larger dimerization than the experimental one [1,35] we restricted ourselves to the SSH model in that work [25] and discussed soliton dynamics within our *ansatz* state as function of soliton width and temperature. In these calculations temperature was included via random forces and dissipation terms. The results were compared to those obtained from the completely adiabatic model and close agreement was found. Reviews of our work on the influence of electron-electron interactions were given in ref. [36].

The application of Heller's formula for the calculation of vibrational spectra from dynamical simulations [37] is shortly discussed in Appendix A in the supplementary material. A discussion on the possibilities to apply our methodology as a general concept in theoretical materials science to predict properties of charge carriers in conjugated polymers together with examples is given in ref. [36] (second paper). Further we mention also there that *ab initio* density functional methods (see for example ref. [38], for semiempirical applications, ref. [39] for applications to polyparaphenylene) can be used to study the stability of such polymers against oxidation in air theoretically. Examples of some of the different functionals developed can be found in refs. [40-45].

The importance of conjugated polymers arises from the fact that they become electric conductors upon doping, with conductivities up to the range of copper (synthetic metals). Further, they are easily processible. The conductivity is usually attributed to a number of different nonlinear quasiparticles as charge carriers, for example, charged solitons, polarons or bipolarons, depending on the nature of the ground state of a given polymer. In some of the materials even the nature of these nonlinear excitations is still controversial. Our general aim is to develop a methodology (see ref. [36], second paper), which is able to produce quantitatively correct answers to questions about form, stability and the motion of such quasiparticles, without using a large amount of computer time or memory. In this way it should be possible to reach theoretical predictions about useful candidates for synthetic metals. Important *ab initio* investigations about the search for low-gap polymers (in different directions regarding the chemical structure) were reported by Bakhshi *et al.* [46-51]. For a comprehensive review of the large amount of work performed by the group of Ladik in this field see ref. [52]. More complete lists of references on this topic, where many more groups are active, can be found in the review of Kivelson, Su, Schrieffer, and Heeger (KSSH) [1] and in our paper on tPA [36].

The present paper is structured as follows. In a first section we want to describe without using any mathematics the basic concept of solitons and polarons in polyacetylene. Then we want to demonstrate that our model is able to explain the experimentally known mobility of neutral solitons in *trans*-polyacetylene as functions of temperature. Following this we want to discuss some static properties of solitons in tPA studied with the help of geometry optimizations. Then we want to give some examples for the dynamics of solitons again in *trans*-polyacetylene and a scenario for the conduction mechanisms derived from these simulations. Further we show that qualitatively correct electronic spectra can be derived from

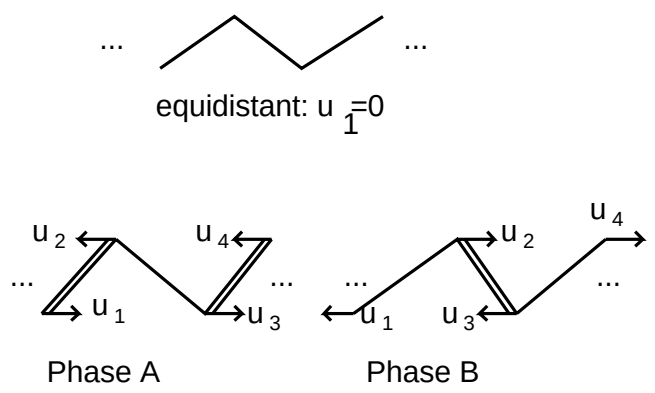

Figure 1 *Sketch of the metallic state and the two degenerate bond length alternation patterns in tPA together with the definition of the displacement coordinates*

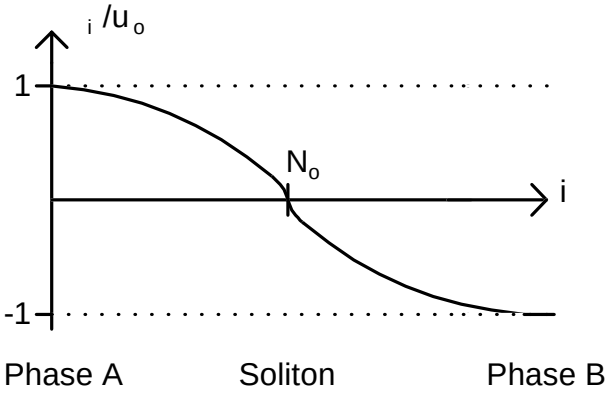

Figure 2 *Sketch of the hyperbolic tangent form of solitons as derived from SSH theory*

these dynamic simulations. Finally in a last section we want to discuss shortly our dynamic simulations on polarons and bipolarons in *cis*-polyacetylene. An outlook on future work will be given in the conclusion. For the details of the theory behind all these calculations we refer the reader to the original literature and to a number of small appendices which can be found in the supplementary material.

The basic concepts of solitons and polarons in polyacetylene

One of the basic facts which had to be explained (see ref. [1] for example) is the presence of an EPR (Electron Paramagnetic Resonance) line with reduced width in undoped samples. This is attributed [1] to the presence of mobile spins (approximately one spin per 3000 CH units) in the pristine material. Further we have a spinless charge transport in lightly doped (<0.06 e/CH) samples and in photoconducting ones. In their famous theory Su, Schrieffer and Heeger (SSH) [1] attributed these features to spinless charged solitons as charge carriers. Their concept of solitons is based on the fact that tPA exhibits two energetically degenerate groundstates, having different bond alternation phases A and B as is shown in Figure 1.

With the help of the local displacements u_i at each site (projected on the polymer axis), phase A can be described by $u_i=(-1)^{i+1}u_0$ and phase B by $u_i=(-1)^{i}u_0$, where u_0 is the so-called dimerization. In fact u_0 is the bond alternation $R_>$-$R_<$ (larger and smaller CC-bond lengths), projected on the polymer axis. The experimental value for u_0 is 0.026 Å (see refs. [53,54] for theoretical calculations and references to experiments therein). SSH introduced the staggered coordinates, $\psi_i=(-1)^{i+1}u_i$, such that the bond alternation phase A can be described by $\psi_i=u_0$ and phase B by $\psi_i=-u_0$. The soliton is then the border between segments of the chain having different bond alternation phases. From SSH theory, which in principle is nothing but a Hückel model extended by a term describing the electron-phonon interaction, it follows [1] that such a soliton centered at a site N_o with a half width L (in lattice sites) is described by a geometry (i denotes the lattice site)

$$\psi_i = u_0 \tanh\left[\frac{N_0 - i}{L}\right] \quad (1)$$

From SSH theory L=7 can be derived. Thus the form of the soliton can be sketched as follows (Figure 2).

From this it is clear that a neutral soliton S^0 carries an unpaired spin, while upon doping a neutral soliton changes to a charged one, which is the charge carrier in the conduction process and has no spin. However, only neutral solitons can be changed to charged ones directly. If a chain which carries no neutral soliton is doped with an electron or a hole, we obtain initially a polaron [1]. Polaron levels have been seen spectroscopically in very lightly doped samples, since polarons show a level structure in the gap which differs sig-

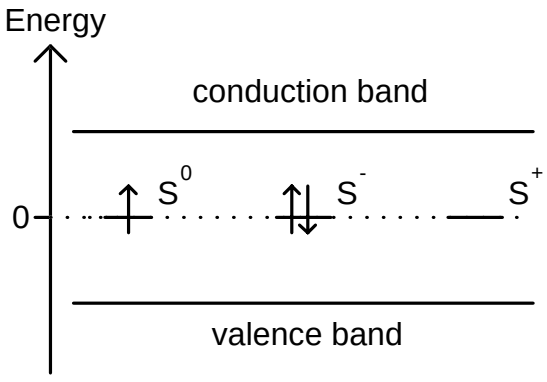

Figure 3 *Midgap levels associated with neutral and charged solitons in tPA as resulting from SSH theory*

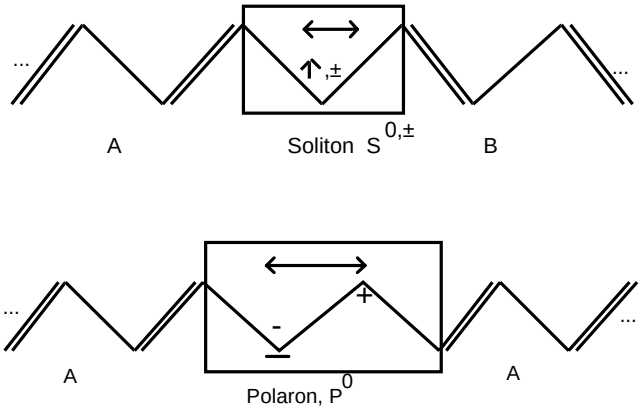

Figure 4 *Idealized sketch of the structures of solitons and polarons (in reality the change in bond alternation phases is smooth)*

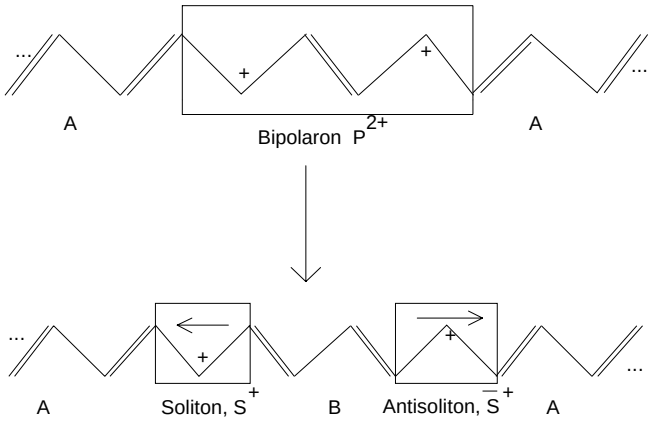

Figure 5 *Idealized sketch of the structure of a bipolaron and its decay into a pair of charged solitons (in reality the change in bond alternation phases is smooth)*

nificantly from soliton levels. In SSH theory all soliton levels appear at midgap (Figure 3).

This is one of the major shortcomings of SSH theory, since experimentally charged solitons are seen below and neutral ones above midgap [2-9]. A soliton and a polaron have the following idealized structures (concentrated on two, respectively, three CC bonds; see Figure 4). In reality the geometry distortion goes over more smoothly to the ideally dimerized phases. Because of the degenerate ground states, the solitons or polarons are rather mobile in the chain. Important is the fact that a soliton has different phases at its two sides, while a polaron connects two identical phases. Thus without a charge on the chain a polaron cannot be stable. If an electron or a hole is added to chains without neutral solitons, a polaron is formed initially and levels in the gap are created.

A further charge will occupy such a level, forming a doubly charged polaron, or bipolaron, which is not stable in tPA and dissociates into a pair of free, charged solitons (Figure 5). A brief explanation of the SSH model and of the method to compute dynamics from this model are given below, while the application of *ab initio* and PPP methods is described in refs. [55-60] and in the Appendices in the supplementary material, with special emphasis on the problem of spin contaminations in UHF calculations.

The Su-Schrieffer-Heeger Hamiltonian (SSH) [1] is given by

$$\hat{H}' = \sum_n \left\{ \left[\beta_0 - (\hat{u}_n - \hat{u}_{n+1})\alpha \right] \sum_\sigma \left(\hat{c}^+_{n\sigma}\hat{c}_{n+1,\sigma} + \hat{c}^+_{n+1,\sigma}\hat{c}_{n\sigma} \right) + \frac{\hat{p}_n^2}{2M} + \frac{1}{2}K(\hat{u}_n - \hat{u}_{n+1})^2 - A(\hat{u}_n - \hat{u}_{n+1}) \right\} \quad (2)$$

In (2) $ß_0$=-2.5 eV is the transfer or resonance integral between two neighbouring CH groups, α=4.8 eV/Å is the electron phonon coupling constant. The values of these constants [1] are determined such that an SSH (Hückel) calculation on an infinite, ordered and ideally dimerized chain results in a π-band width of 10 eV and a fundamental gap of roughly 2 eV. M=13 m_p (in ordered chains) is the mass of a CH unit, K is the spring constant due to the σ-electrons between two neighbouring units. K and the linear potential constant A are determined such, that the ideally dimerized chain shown in the following sketch (Figure 6) represents the equilibrium geometry of the chain [26]. As shown in detail in Appendix F in the supplementary material, in the adiabatic approximation the CH units are considered as classical particles moving in the potential created by the π-electrons and harmonic terms due to the σ-electrons, which form a system of localized CC-bonds, underlying the delocalized π-system.

In Figure 6, the u_n are the projections of the displacements of the CH units from the equidistant chain onto the polymer axis, a_0 is the lattice constant of the equidistant chain and y_0 is the distance of the CH units from the chain axis, which is kept constant in the SSH model. a_0 and y_0 are determined such that the long CC bond in equilibrium has a length of 1.450 Å, that the short CC bond one of 1.366 Å and that the CCC angle has a value of 123.9°, a geometry which was obtained with the help of correlated *ab initio* calculations on

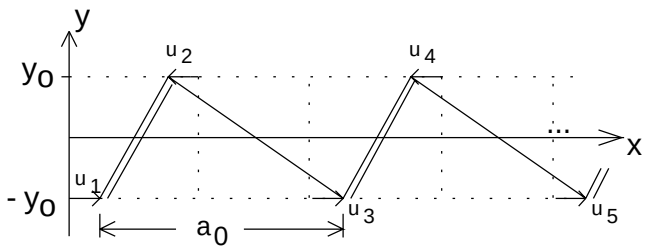

Figure 6 *Sketch of the geometry and the coordinates we use for our simulations on trans-polyacetylene*

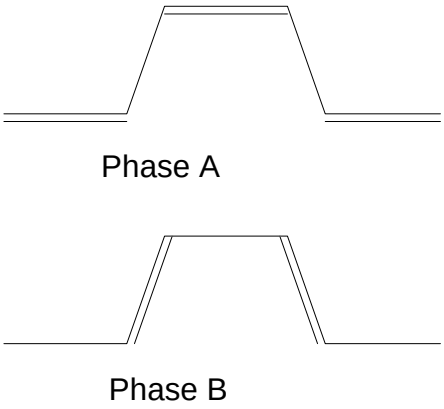

Figure 7 *Sketch of the two different bond alternation phases in cis-polyacetylene*

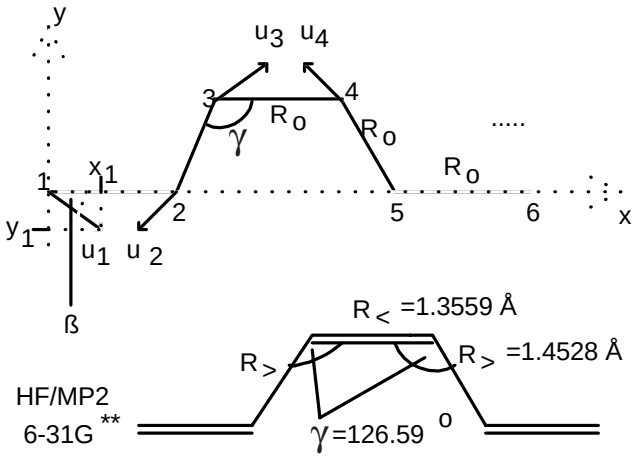

Figure 8 *Definition of the displacement coordinates in cis-polyacetylene and the correlated ab initio geometry (6-31G** basis set, MP2 method) of cis-hexatriene*

the infinite chain by Suhai [61-64]. $\hat{u}_n$ is the operator of the displacements of the units parallel to the chain axis from their positions in the equidistant chain, and $\hat{p}_n$ the corresponding momentum operator. The operator $\hat{c}^{+}_{n\sigma}$ ($\hat{c}_{n\sigma}$) creates (annihilates) an electron with spin orientation σ at unit n. In *trans*-polyacetylene (t-PA) as can be seen from the above sketch two energetically degenerate bond alternation phases exist. In chains with an odd number of carbons we have an unpaired electron, which occupies a nonbonding level at midgap, the soliton level. The soliton is a domain wall where the system switches from one bond alternation phase to the other. Details of the time simulations in the usually used adiabatic model are given in Appendix F in the supplementary material. In this case, using the SSH Hamiltonian, one observes a stable and mobile soliton [1].

Turning now to *cis*-polyacetylene the two local minima of the bond alternation phase can be sketched as follows in Figure 7. Obviously in this case the two bond alternation phases are not energetically degenerate: phase B is higher in energy than phase A. Since the two phases are not degenerate, a soliton would result in a chain (of a length of n+m units) of the idealized form $(A)_n$-$(B)_m$ which is unstable against the form $(A)_{n+m}$. Thus solitons cannot be formed in this material.

However, here polarons would be stable, because dependent on the width of the polaron the length of the B-segment could be kept small: $(A)_n$-$(B)_{n'}$-$(A)_m$. Further in polarons the central region of the polaron does not exhibit a fully formed B-phase but rather a bond alternation which resembles more the equidistant structure. Spinless charge carriers in the system would then be bipolarons, i.e., doubly charged polarons. The length of the B-segment, i.e. the width of the bipolaron would then be determined by the repulsion of the two equal charges and it would not decay into a central breather and two separated charged solitons as is the case in tPA. The width would be determined by the interplay between two effects:

(i) The repulsion of the two charges would favour a large B-segment $(B)_{n'}$

(ii) Since the formation of the B-segment is energetically unfavourable, the electron-phonon coupling would tend to keep it small.

To apply our procedure to this system, we have to define a coordinate which switches from the A-phase to the B-phase based on a geometry optimization of *cis*-hexatriene. The results are shown in Figure 8. Results of our simulations on *cis*-polyacetylene (cPA) are shown below. Now we want to turn to the dynamics of tPA.

Temperature dependence of the mobility of neutral solitons in tPA

Temperature is included in our treatment via Langevin equations (see Appendix A in the supplementary material) for the lattice. For this study we applied an exact solution of the time dependent Schrödinger equation for the special case of the SSH Hamiltonian with a classical lattice (see Appendix A in the supplementary material for details). Since Langevin equations are strictly correct only for classical systems, our results for very low temperature (T=10 K) are approximative. We had to use a very small time step size of 0.01 fs, because the electron dynamics are much faster than the lattice dynamics. In the calculations discussed so far, it was always assumed, that the electrons follow the lattice motions instantaneously, thus a time step of 1 to 1.25 fs was sufficient. Since in our study we want to simulate PPP results as accurately as possible with our exact SSH solution (Appendix A in the supplementary material), we have to choose β_0=-2.5 eV and α=4.8 eV/Å. The value of u_0 has to be chosen such that it is smaller than the experimental one, because from PPP and MINDO calculations it is known that the soliton width L is

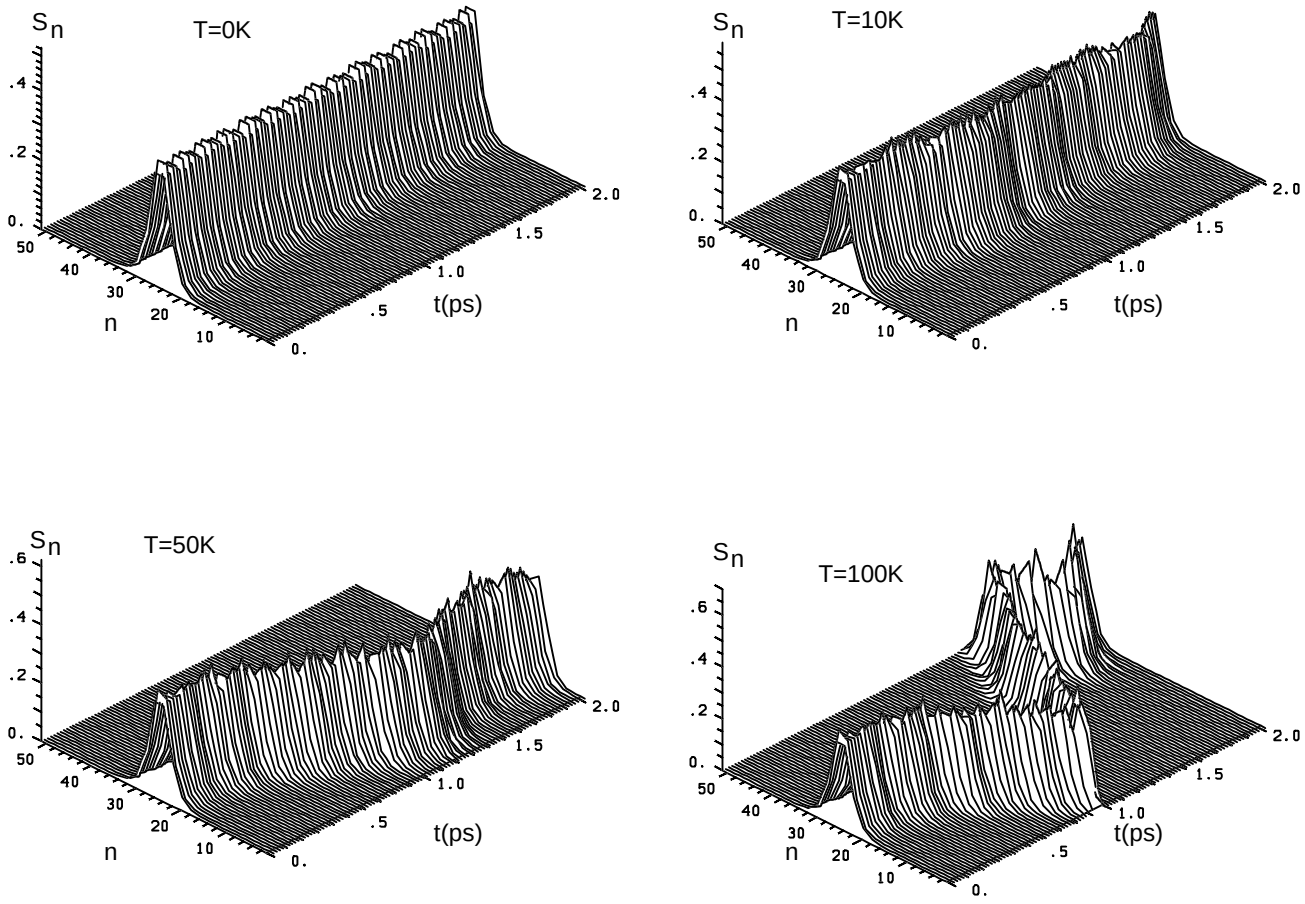

Figure 9 *Results of simulations using the exact solution of the classical SSH Hamiltonian (see Appendix A): Spin density (α-spin) on odd numbered sites (those on even sites are vanishing) S_n as functions of site n and time t.We used a neutral chain with 51 units (K=17.0100 eV/Å², A=-5.68346 eV/Å, Γ= 1.09744 ps⁻¹) and a soliton of tanh-shape with L=3 and N_0=26 as initial state (β_0=-2.5 eV, α=4.8 eV/Å, u_0=0.1 Å, time step 0.01 fs) at T=0K, 10K [σ= 0.256657 (eV/Å)²], 50K [σ= 1.28328 (eV/Å)²], 100K [σ= 2.56657 (eV/Å)²]*

roughly equal to 3 lattice sites. However, the SSH Hamiltonian with experimental u_0 values gives soliton half-widths around 7 lattice sites. To obtain the desired soliton width of 3 sites, we used u_0=0.1 Å. We placed initially a soliton of tanh-shape with L=3 and centered at N_0=26 into a neutral chain of 51 units. The initial values for the time dependent MO coefficients were obtained from a conventional static SSH calculation on the system with the initial geometry. Then we performed time simulations using the above derived formalism at different temperatures, namely T=0 K, 10 K, 50 K, and 100 K. For the four different temperatures the evolution of the total energy (being simply an error at T=0 K) and of the kinetic energy was inspected. The error at 0 K was still quite large; however, it was negligible compared to the thermal energies. Furthermore, simulations with 0.001 fs as time step showed that the result is the same as with the larger one. In plots of the staggered lattice displacements besides the tanh-shape of the soliton the thermal fluctuations are clearly visible. The most interesting plot is shown in Figure 9, namely the spin densities on odd numbered sites. We see clearly that the soliton is completely immobile at 0 K. At 10 K a very small shift in position seems to occur. Then at 50 K temperature obviously the soliton is able to move more or less randomly in the chain, though, only from the center of the chain to its end. At 100 K, finally the soliton becomes freely mobile and moves due to the effect of temperature through the complete chain. In Appendix B in the supplementary material the relation of our method with the $|D_2>$ state is discussed in detail.

This result agrees with experiments, where it was found that between 10 K and 100 K the behaviour of neutral solitons in tPA changes from being completely immobile below 10 K to completely mobile above 100 K. Between these temperatures a continous transition is observed. This is exactly the behaviour that we expect from our theoretical calculations.

Applications to tPA chains and the calculation of electronic spectra

In our applications to tPA we want to distinguish between static calculations involving geometry optimizations, which we perform with our time simulation program by setting the lattice velocities to 0 after each time step. In this way we obtain simply a gradient optimization scheme. However, we can also multiply the velocities with a factor between 0 and 1 after each time step. In this way the lattice is cooled down slowly, and the system can override some local minima which are higher in energy than the total minimum. Further, we want to show the results of some of our dynamic simulations. However, since the material was published already previously [36], we want to keep the discussion short, concentrating on the most important results. A description of methods is given in Appendix C in the supplementary material.

Static properties

First of all we have to note here that in optimization procedures with the AUHF method the optimum half width of neutral solitons converges with increasing chain length N to a half width of 2.5 lattice sites, while with UHF it diverges. Further, we want to note that a half width of neutral solitons of around 3 lattice sites is in agreement with results of Boudreaux *et al.* [16] obtained using a semiempirical all valence electron (MNDO) method and a Restricted Open Shell HF (ROHF) scheme. In these calculations, instead of applying a DODS (Different Orbitals for Different Spins) method like UHF, EHF or AUHF, one uses a simple RHF scheme, with occupation numbers of 0, 1 or 2 (instead of 0 or 2 in RHF for closed shells). However, our AUHF method now leads to the correct expectation values of the square of the spin operator for doublets. In chains with 101 units and an optimized soliton in the center of the chain, UHF converges to a solution which shows $< \hat{S}^2 >=10.8\ h^2$ instead of the correct value for a doublet state of $3/4\ h^2$ which is obtained with the AUHF method. Further, we obtain a spin polarization with both methods as it was found with ENDOR experiments. However, with UHF the spin density wave is undamped, and the averaged values of the spin densities on consecutive sites are far too large. AUHF yields values in the correct range, but it underestimates the spin polarization slightly. We used a chain of 41 units (the conjugation length in Shirakawa samples of tPA is roughly between 20 and 40 double bonds) and computed the average spin densities S separately for odd numbered (S_o) and even numbered (S_e) sites for the UHF and the AUHF method and compared these numbers with the high temperature ENDOR results (measured spin densities are time averaged by soliton movement). The results we obtained are:

ENDOR	$S_o = +0.06$	$S_e = -0.02$	alternating
AUHF	$S_o = +0.05$	$S_e = -0.01$	alternating
UHF	$S_o = +0.40$	$S_e = -0.40$	alternating

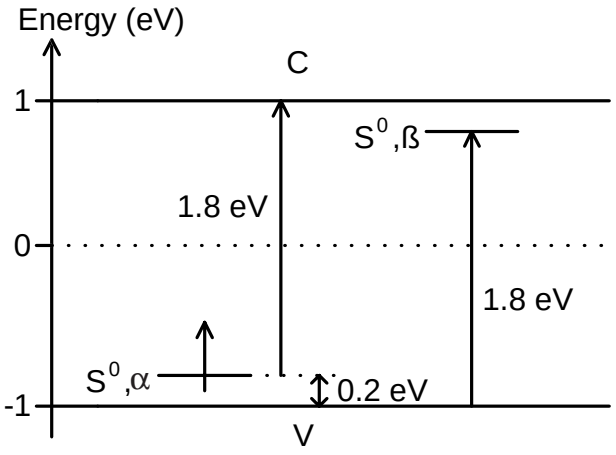

Figure 10 *Position of the energy levels of a neutral soliton in the gap of tPA (all energies scaled such that the gap is 2 eV) calculated with the AUHF method*

It is obvious that the UHF method shows far too large spin contaminations to yield a reliable description of tPA, while the error obtained with AUHF is tolerable. Further, we compared AUHF spin densities in a C_9 and a C_{11} chain with results obtained by Soos and Ramasesha [60] with an exact digonalization of the Hamiltonian which is possible for such small systems. However, note that even with the faster computers available nowadays exact diagonalizations are still far from possible for chains of realistic lengths (30-100 units), especially in time simulations where the procedure (for example, the Lanczos method) would have to be repeated in each time step. Although our comparison showed that the spin density wave in the AUHF method is somewhat more strongly damped than in exact diagonalizations, and as shown above the spin polarization becomes underestimated, the results are still reliable. On the contrary, the UHF results are completely unrealistic.

The following sketch (Figure 10) shows the energy levels in the gap due to a neutral soliton of width 2.5 in a chain of 121 units, as obtained with the AUHF method and scaled such that the value of the gap is 2 eV, which corresponds to the experimental value of the fundamental gap in tPA. Clearly the AUHF excitation energies as such are far too large as, is usually found in HF calculation. Further, there is no reliable way to obtain correlation corrections to AUHF energy levels. In addition, UMP (perturbation theory based on an UHF reference) calculations are known to be rather questionable on *ab initio* level and our experiences with *ab initio* applications show that such scaling procedures are not unrealistic. Thus we are quite confident that the level distribution shown in our sketch based on scaled AUHF calculations is a quite reasonable one. Note that the S^0 levels (neutral soliton) split into an occupied α-spin level close to the valence band and a virtual β-spin level close to the conduction band. However,

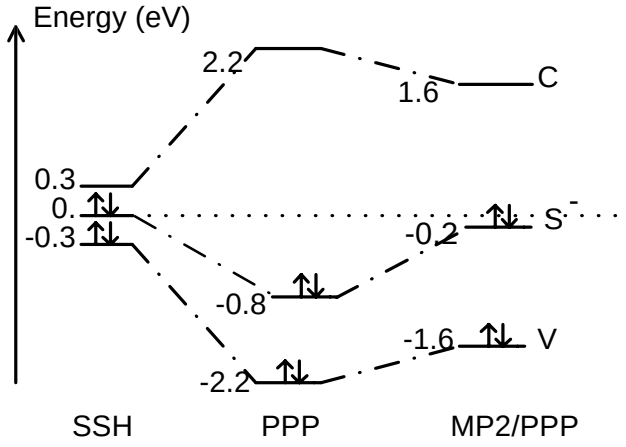

Figure 11 *Positions of the energy levels associated with a negatively charged soliton in the gap of tPA calculated with different methods (see text)*

both levels are connected with the same excitation energy of about 1.8 eV.

This scaled excitation energy is still too large compared to the photoinduced high energy absorption [2-4] found at 1.35 eV; however, it lies in the correct range, close to the band edge. Note that we parametrized our PPP Hamiltonian with respect to potential surfaces. Therefore, excitation energies still would need the usual correlation corrections.

For the study of charged solitons we chose a chain of 81 units length and a negatively charged soliton of width L=8 lattice sites in its center. The sketch below (Figure 10) shows the PPP-HF results which clearly indicate that the gap obtained is too large (4.4 eV), while the negative soliton level lies 0.8 eV below midgap instead of above as the photoinduced low energy absorption suggests. However, since here we have to deal with a closed shell system we could apply the usual correlation corrections to the energy levels, for example, Suhai's method [61-64] for polymers, which can also be applied for molecules (see for example ref. [62]). In this method the self-energies added to a level i (occupied) or r (virtual) can be calculated on second order perturbation theory (MP2) level as explained in Appendix D in the supplementary material.

Then the correlation corrected energy levels denoted by ε_i and ω_r, respectively, are calculated again following Appendix D in the supplementary material (based on an extended version of Koopmans' theorem [52,61-64]). Note, that the results given in ref. [36] were obtained with AO integrals not corresponding to the Ohno parametrization mentioned above, which seems to be the best one for tPA. With this method we obtain a gap of 3.2 eV which compares very well with Suhai's best basis set *ab initio* result of 3 eV [61-64]. Now the negatively charged soliton level appears close to midgap as in SSH theory (-0.21 eV).

However, in our case the excitation energy is not given simply as the difference of the energy levels, but has to be

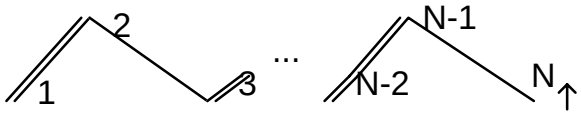

Figure 12 *Sketch of the end-kink geometry used for our simulations as initial configuration (chain with an odd number of CH groups in phase A)*

corrected with the coulomb- and exchange integrals (-0.44 eV correction to the simple differences of state energies) between the occupied and the virtual level taking part in the excitation process. This value is well below midgap as expected from experiment. This excitation energy from the soliton level to the conduction band amounts to 1.35 eV, or scaled such that the gap is 2 eV (factor 2.0/3.2), the excitation energy is 0.9 eV. Thus we can summarize our results obtained with the new parametrization as follows (N is the chain length):

Excitations:

$S^0 \rightarrow C$, $V \rightarrow S^0$:	1.8 eV	exp.: 1.35 eV
$S^- \rightarrow C$, $V \rightarrow S^+$:	0.9 eV	exp.: 0.45 eV

Soliton widths (PPP):

$L(S^0)$ = 2.5 sites	MNDO: 3 sites
$L(S^{\pm})$ = 5.9 sites (N=21)	*ab initio*: 6 sites (N=21)
$L(S^{\pm})$ = 10 sites (N=121)	converged with increasing N

Dynamical simulations

In our dynamical simulations we obtained results which are close to experimental facts. We want to present here dynamics of neutral and charged solitons (see Appendix C in the supplementary material for the method). Further, we want to discuss the dynamics of singly charged even numbered chains, where according to experience polarons are formed. In addition we study doubly charged even numbered chains where bipolarons should not be formed but free pairs of charged solitons which repel each other. Further, we calculated dynamics of excited states, and of disordered chains. For simulations on even numbered chains we start with an ideally dimerized chain, while for those on odd numbered chains we start with an end-kink configuration (in both cases $\psi_n(t=0)/u_0 = 1$; see Figure 12 below). From initial configurations like that, mobile solitons are formed, because a localized spin or charge prefers to be situated in the center of the chain, and it polarizes the lattice around it to form a solitonic configuration.

In Figure 13, we show the spin density on odd numbered sites only (to avoid the oscillations between consecutive sites due to spin polarization in the plot) for an initial end kink configuration in a chain of 31 units using the AUHF method and our alternative *ansatz* for the σ-potential (see Appendix

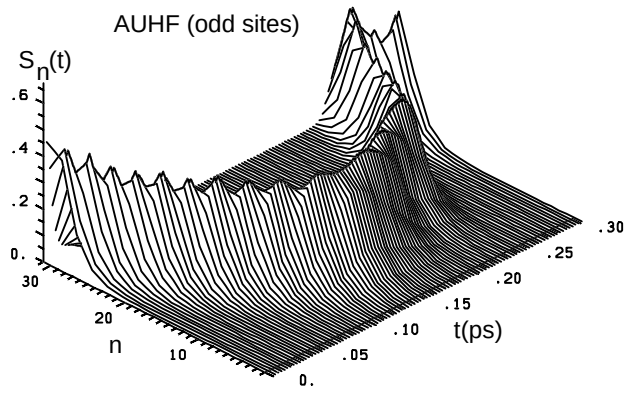

Figure 13 *Spin densities (α-spin) $S_n(t)$ at odd numbered carbons in a neutral chain of 31 units (u_0=0.0238 Å, a_0=1.2428 Å and y_0=0.3307 Å) and starting from an end kink configuration ($\psi_n(t=0)/u_0=1$) as function of site n and time t (the time step is 1.00 fs), using the AUHF (K=35.070 eV/Å^2, R_0=1.507 Å) method*

C in the supplementary material). Obviously the spin localized at the chain end moves away from it and travels through the chain with a more or less uniform velocity, which amounts to 2.9 km/s, much smaller than in the SSH case. This is a direct consequence of the smaller width of the soliton, since the smaller the width of the soliton, the more it tends to lattice pinning. Note, that although the width of the soliton in the lattice is quite small (roughly 3 sites), the spin density wave associated with it extends over more sites, in fair agreement with experimental results [65], where the form of this wave could be directly measured. Figure 14 shows the dy-

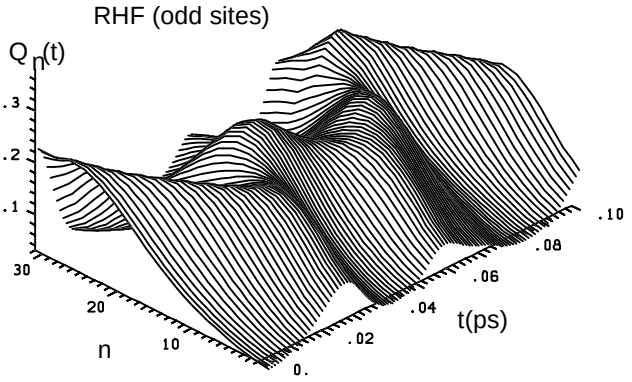

Figure 14 *Charge densities $Q_n(t)$ at odd numbered carbons in a singly charged (positive) chain of 31 units (u_0=0.0238 Å, a_0=1.2428 Å and y_0=0.3307 Å) and starting from an end kink configuration ($\psi_n(t=0)/u_0=1$) as function of site n and time t (the time step is 1.00 fs), using the RHF (K and R_0 determined with AUHF on the corresponding uncharged chain, values as in Fig. 13) method*

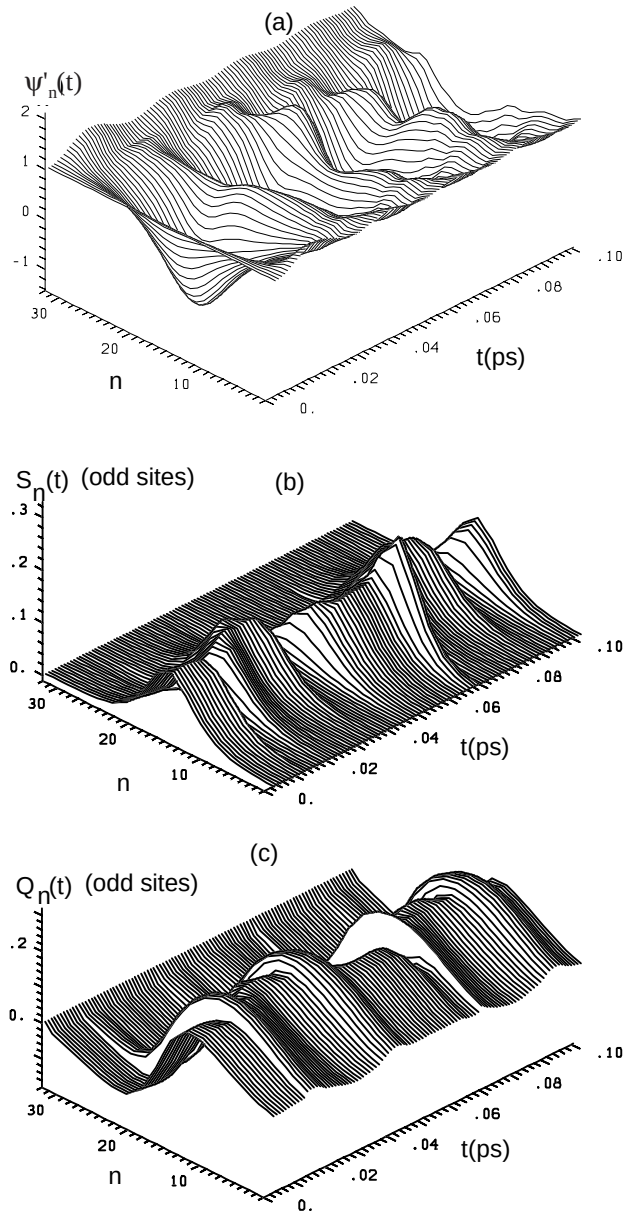

Figure 15 *The normalized staggered lattice displacements (***a***)*

$$\psi'_n(t) = \frac{1}{(4-2\delta_{n1}-2\delta_{nN})u_0}\left\{\left[\psi_n(t)+\psi_{n-1}(t)\right](1-\delta_{n1}) + \left[\psi_n(t)+\psi_{n+1}(t)\right](1-\delta_{nN})\right\}$$

*the spin densities (α-spin) $S_n(t)$ (***b***) and the charge densities $Q_n(t)$ (***c***) at odd numbered carbons in a singly charged (positive) even numbered chain of 32 units (u_0=0.0238 Å, a_0=1.2424 Å and y_0=0.3311 Å), starting from uniform dimerization ($\psi_n(t=0)/u_0=1$) as function of site n and time t (the time step is 0.25 fs), using the AUHF (K=39.514 eV/Å^2, R_0=1.495 Å, determined in the corresponding uncharged chain using RHF) method*

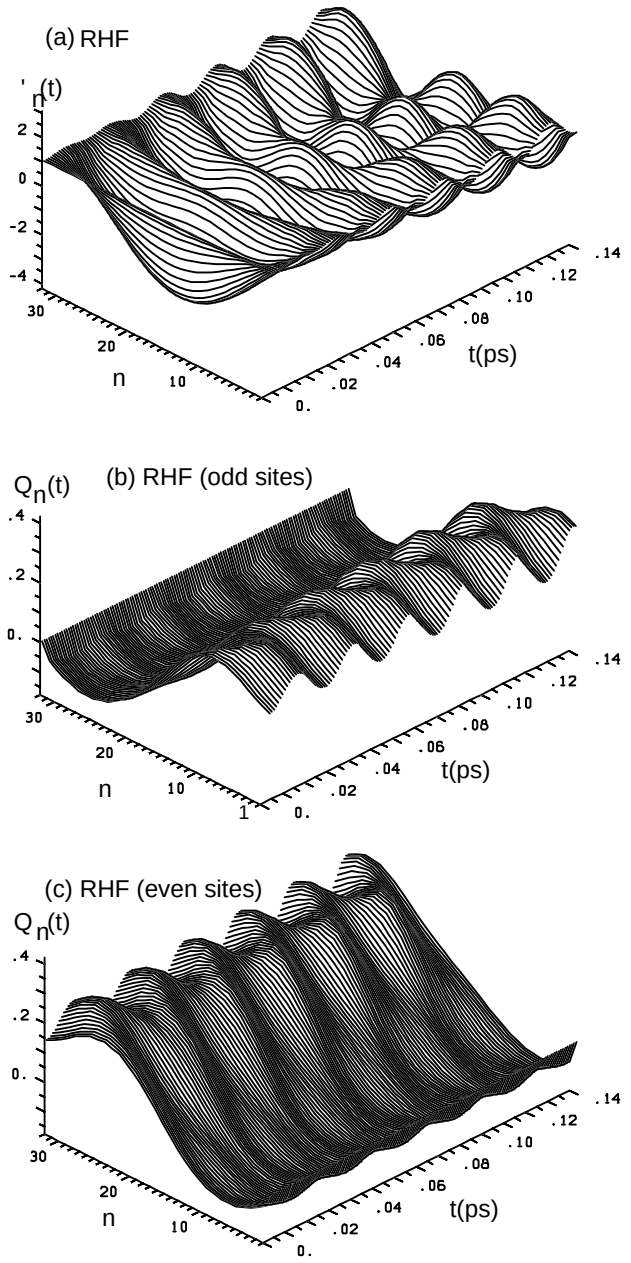

Figure 16 *The normalized staggered lattice displacements (***a***)*

$$\psi'_n(t) = \frac{1}{(4-2\delta_{n1}-2\delta_{nN})u_0}\left\{\left[\psi_n(t)+\psi_{n-1}(t)\right](1-\delta_{n1})+\right.$$
$$\left.+\left[\psi_n(t)+\psi_{n+1}(t)\right](1-\delta_{nN})\right\}$$

*and the charge densities $Q_n(t)$ at odd (***b***) and even (***c***) numbered carbons in a doubly charged (positive) even numbered chain of 32 units (u_0=0.0238 Å, a_0=1.2424 Å and y_0=0.3311 Å), starting from uniform dimerization ($\psi_n(t=0)/u_0=1$) as function of site n and time t (the time step is 1.00 fs) calculated with the RHF (K=39.514 eV/Å^2, R_0=1.495 Å, determined in the corresponding uncharged chain using RHF) method.*

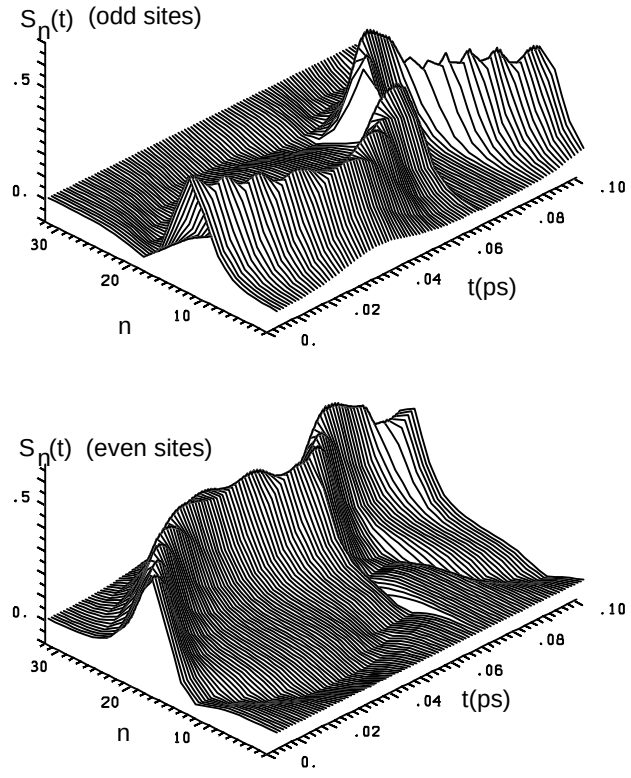

Figure 17 *Spin densities (α-spin) $S_n(t)$ at odd and even numbered carbons in a neutral even numbered chain of 32 units (u_0=0.0238 Å, a_0=1.2428 Å and y_0=0.3307 Å) starting from uniform dimerization ($\psi_n(t=0)/u_0=1$) as function of site n and time t (the time step is 0.125 fs), after an initial ^3B_u excitation (m=1) using the AUHF (K=39.492 eV/Å^2, R_0=1.495 Å, determined for the corresponding ground state using RHF) method*

namics of a singly charged (doped) odd numbered chain, where the excess charge occupies the soliton level and a charged soliton or charge carrier is formed.

Figure 14 shows the charge distribution on odd numbered sites for a positively charged soliton in a chain of 31 units. It is clear from the Figure that the width of the charged soliton is larger than that for a neutral one, and consequently it has a larger velocity (18 km/s). In Figure 15a we show the time evolution of the staggered lattice coordinate for a singly charged even numbered chain. It is clear that in this case no free solitons are found. On the contrary, the lattice distortion in the center of the chain relaxes to a minimum value larger than $-u_0$, while a B-phase segment would show distortions smaller than $-u_0$, because due to the excess energy a B-phase in the chain would be overshooted. In contrast here we have a typical polaron structure, with a distortion of 0 in its center, slightly overshooted due to the excess energy over polaron binding energy the chain gains by putting an extra charge into its electronic structure (an electron into the conduction band or a hole into the valence band). In our case we re-

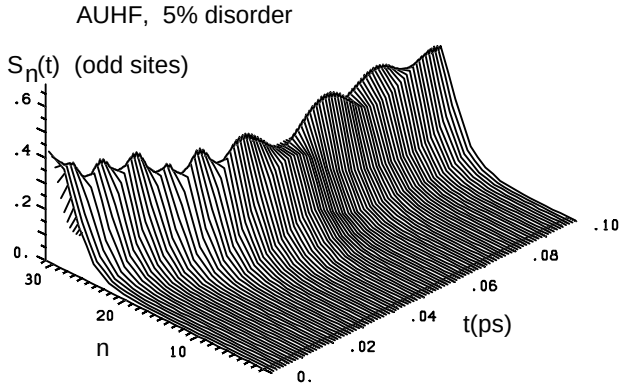

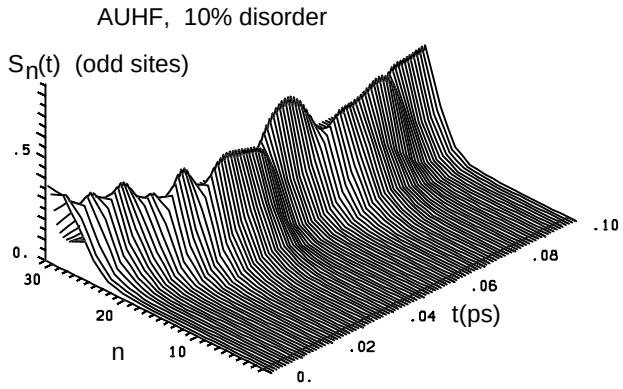

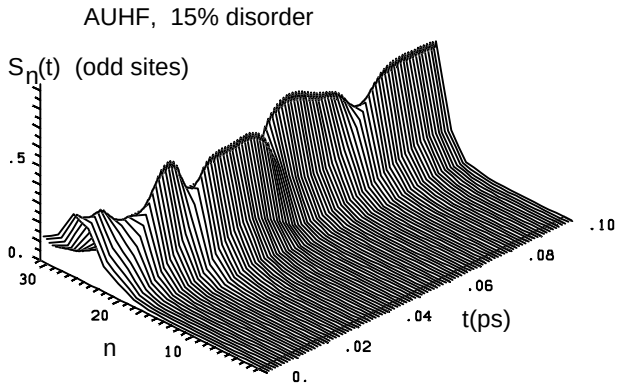

Figure 18 *Spin densities (α-spin) $S_n(t)$ at odd numbered carbons in a neutral chain of 31 units (u_0 = 0.0238 Å, a_0 = 1.2428 Å and y_0 = 0.3307 Å) with a random distribution of the electronic parameters. x is the maximum value of the disorder x_n ($-x<x_n<x$) given in % of the normal values of the parameters: $\alpha_n = \alpha(1+x_n)$, $\beta_{0,n} = \beta_0(1+x_n)$ and $I_n = I(1+x_n)$ (the ionization potential). Note, that for the γ-s we use here:*

$$\gamma_{nm} = \frac{V}{\sqrt{\left(\frac{V}{d_{nm}}\right)^2 + R_{nm}^2}}; \quad d_{nm} = \frac{1}{2}\left(I_n - A_n + I_m - A_m\right);$$

$$V = \frac{1}{4\pi\varepsilon_0}$$

where $A_n = A(1+x_n)$ is the electron affinity. Here we use I = 11.54 eV and A = 0.46 eV. x_n is a random number between -x and x and we start the simulations from an end kink configuration ($\psi_n(t = 0)/u_0 = 1$). The spin densities are given as function of site n and time t (the time step is 1 fs), using the AUHF method for three different disorder strengths, namely x = 0.05 (K = 34.2878 eV/Å², R_0 = 1.5084 Å), x = 0.10 (K = 33.2322 eV/Å², R_0 = 1.5115 Å) and x = 0.15 (K = 27.9892 eV/Å², R_0 = 1.5307 Å)

moved a charge from the valence band. Due to this excess energy, the polaron oscillates back nearly to the undistorted chain and is formed again afterwards. Also the spin (15b) and the charge density (15c) show a typical polaronic structure. This result is in fair agreement with experiment, since in very lightly doped samples the spectral features of polarons were found. Figure 16 displays the dynamics which evolve from an even numbered chain of 32 units with two positive charges. In contrast to the singly charged chain, here a well developed B-phase segment occurs between the two separating charged solitons.

However, this structure decays into a breather vibration between the solitons. Each soliton moves between its respective chain end and the center of the chain, as the plot of the charge density on odd numbered sites indicates, while the central breather remains stable. The charge density on odd numbered sites shows one of the positively charged solitons, while the other one has its charge on the even numbered sites. If the chain would be longer, the two charged solitons would separate completely, leaving the breather vibration between them. Thus a scenario for doping would be, that initially for very small dopant concentration in even numbered chains charged polarons would be formed. These polarons create levels in the gap. Thus the electrons from further doping will occupy such gap levels and form unstable bipolarons which would decay into two free, separating charged solitons and a central breather vibration between them. This is in qualitative agreement with experimental findings and conclusions from calculations with the SSH Hamiltonian [1-4].

Figure 17 shows the α-spin density on odd numbered sites as a function of time which developes from an even numbered chain after a m=±1 triplet excitation. We have chosen this kind of excitation, because it can be described with one Slater determinant. Thus we can use an AUHF simulation, where we just changed the occupation numbers for the different spins accordingly. Namely, we removed one β-spin electron and placed it into the first virtual orbital of α-spin. The plot shows clearly that two neutral solitons are formed, which move in their respective halves of the chain. The second soliton would show up in a plot of the spin density on even numbered sites. A similar situation, however, with charged solitons forming from the initial excitations we found for ^1B_u states which have to be described by at least two Slater

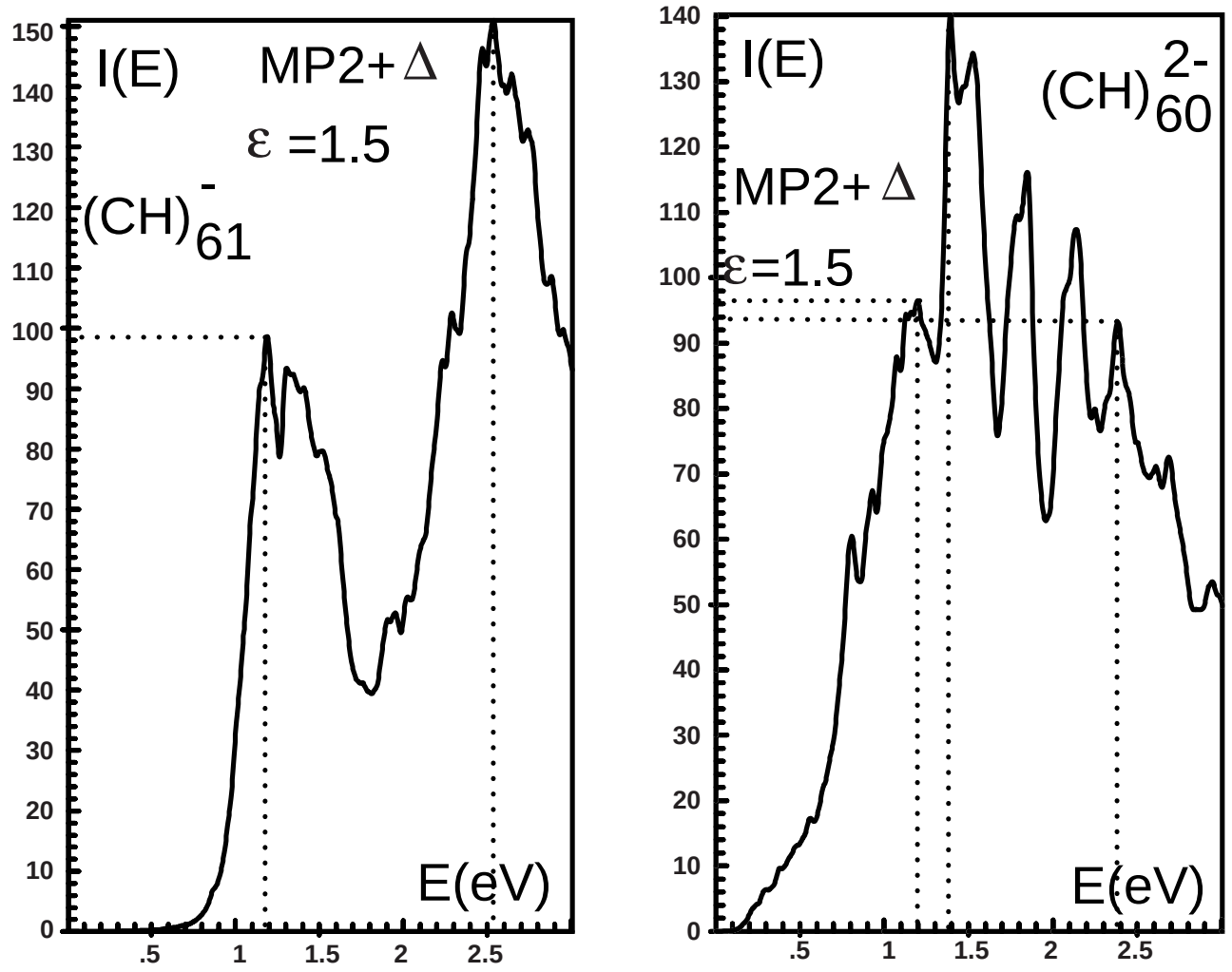

Figure 19 *Electronic spectra of an odd numbered chain of 61 units with one negative charge (left panel) and of an even numbered chain of 60 units with two negative charges (right panel), calculated as described in the text and in Appendix D in the supplementary material. The vertical lines indicate the soliton peak and the band to band excitation. The intensities I(E) are in arbitrary units (corresponding to the equations given in Appendix D in the supplementary material)*

determinants [66]. An MCSCF formulation for singlet excited states has been developed and presented in our previous paper [67].

Another interesting case is the behaviour of neutral solitons in disordered chains. The generally accepted scenario for the origin of the high energy photoinduced absorption is the assumption that it originates from neutral solitons. However, by a ^1B_u excitation only charged solitons are created via the lattice polarization due to the initially created electrons in the conduction band and holes in the valence band. In the usual SSH or PPP Hamiltonians these excitations cannot be converted to neutral solitons. However, Kivelson *et al.* [7b] could show, that already second neighbour interactions in the one-electron part of the Hamiltonian of very small strength make the reaction $S^+ + S^- \rightarrow 2S^0$ allowed and probable. The temperature dependence of the high energy absorption is then explained with a confinement of the neutral solitons in disordered regions of the chain, which would prevent them from recombination. Increasing temperature then could help the solitons to escape from their traps and recombine. Thus it remains to be shown that disorder can really function as a trap for neutral solitons. For this reason we performed simulations in neutral odd numbered chains (31 units) with a random sequence of values for the electronic parameters α, β_0, γ_0, and the on-site ionization potential I. We allowed fluctuations around the usual values of the parameters within a given percentage deviation. Simulations of this type are shown in Figure 18. Indeed we found that even small fluctuations in all three parameters (maximum of ±5% of their normal values), are sufficient to hinder the soliton motion as our Figure shows. With ±5% and ±10% disorder in the chains the soliton

motion is restricted to a small number of sites, while with ±15% disorder the soliton becomes completely trapped, which is consistent with the assumed scenario for the high energy absorption.

Electronic spectra

The method for the calculation of electronic spectra from our dynamical simulations of polyene chains is outlined shortly in Appendix D in the supplementary material. In Fig. 19 we show the spectra which we obtained from simulations on chains containing 61 CH units with one negative charge and with 60 CH units and two negative charges (both simulations started from the same end-kink geometry).

The figure clearly indicates that qualitatively our method reproduces the experimental spectra quite well. Note, that in experimental spectra the structure showing a lot of sharp minima and maxima is mostly smoothed out via couplings to phonons and to the environment of the chains. Further the limited chain lengths used in our calculations might play a role in the creation of this artefact. However, there is still one basic shortcoming in our results. Namely, the peaks are consistently too high in energy. For the soliton peaks we expect from experiment a frequency corresponding to roughly 0.8 eV, while we obtain 1.2 eV for the singly charged soliton and a side peak at again 1.2 eV in the doubly charged case, while the peak of the soliton absorption in the latter case is at 1.4 eV in our theoretical spectrum. The band to band excitation peaks at 2.5 eV in the singly charged case, while we identify the side peak at 2.4 eV in the singly charged case as the band to band excitation. The other side peaks correspond to excitations from the soliton levels to the conduction band. Thus our frequencies are all by about 0.3-0.5 eV too high in energy. However, the reasons for that are well defined and are under study in the moment:

(i) The level of electron correlation included in the calculations (MP2, see Appendix D in the supplementary material) might be too low for the present purpose. We are going to implement MP3, the third order of perturbation theory currently to be able to investigate if this is the reason for the error or not.

(ii) The exciton corrections (in HF and conventional MP2 calculations of energy level differences the interactions between the electron in the conduction band and the hole in the valence band or the soliton levels is neglected) are calculated with the help of the HF wave function only, not with the correlated one.

(iii)Since we do not treat the σ-electrons explicitely in our method, we had to include a relative dielectric constant ε in $V=e^2/(4\pi\varepsilon_0\varepsilon)$ and also in $\gamma=\gamma_0/\varepsilon$, where γ is the on-site electron-electron repulsion strength. In this work we use ε=1.5, which is commonly used [68] and appropriate for polydiacetylenes [52,61-64]. It might well be that for polyacetylene another value of ε would be better suited, although our calculations on neutral chains indicate that with ε=1.5 the band to band excitation peaks correctly at 2 eV.

(iv) A chain length of only 30 double bonds could be too small as compared to experimentally occurring levels. Further, in a real sample propably a distribution of chain lengths should be present. The short chain length leads to a compression of the charged solitons, which have a rather large width also in the PPP model, resulting from the chain ends, being too close to each other. Such a compression of the solitons, especially when there are two of equal charge present on one chain, could shift the frequencies to higher energies.

Our theoretical spectra show clearly the bleaching of the band to band absorption with increasing doping level. The bleaching rate in the calculated spectra suggests a doping level as expected from comparison with experiment (see below). In $(CH)_{61}^-$ the doping level is y=1/61 charges per CH unit which is approximately equal to 0.017. We measured the ratio x of the intensity at the peak maximum of the soliton excitation at around 0.8 eV to the peak maximum of the band to band excitation at 2 eV in the corresponding Fig. 34 from ref. [1], which was reprinted there from ref. [69], showing the spectra for polyacetylene as function of the (electrochemical doping) cell voltage. Using the heights of the maxima of the band to band absorptions measured from the figure, we obtained the corresponding doping levels with the help of an expression given by KSSH [1] (see Appendix D in the supplementary material). In Fig. 20 we show a plot of the doping level y versus the ratio x, measured from Fig. 34 in ref. [1]. From our spectrum for $(CH)_{61}^-$ we obtain x from the intensities at 1.2 eV and 2.5 eV, respectively, as 0.645. As shown in Fig. 20 this value of x suggests a doping level of around y=0.021, which is in fair agreement with the actual value of 0.017. With the intensities measured for $(CH)_{60}^{2-}$ at

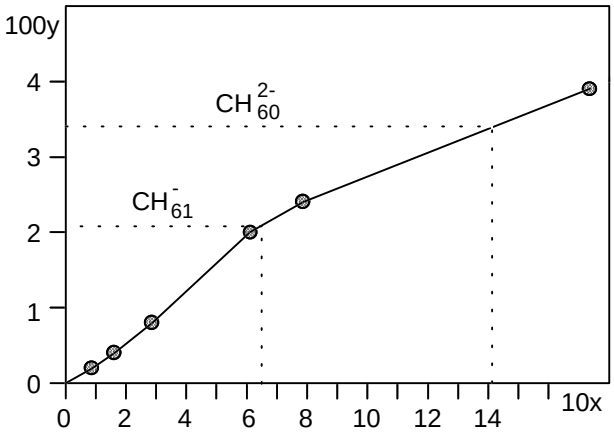

Figure 20 *The doping level y from Table 1 in Appendix D in the supplementary material (in charges per CH unit) plotted against the ratio x of the experimental height of the soliton peak at around 0.8 eV to the experimental peak hight of the band to band to band transition at 2 eV in doped polyacetylene as measured (shaded circles) from Fig. 34 in ref. [1] (reprinted from the results published originally by Feldblum et al. [69]). The dashed lines correspond to the measured values of x from Figure 19*

1.4 eV and 2.4 eV, respectively, we obtain x=1.409 and thus a doping level of y=0.034, in excellent agreement with the actual value of y=2/60 charges per CH unit.

In Figure 21 we show finally the photoinduced spectrum obtained from a simulation on the first excited singulet state ^1B_u for $(CH)_{60}$. Here the situation is clear. The soliton excitation peaks at around 0.7 eV, again by roughly 0.3 eV too high in energy as compared to the experimental value. We do not expect an artificial compression of the resulting charged solitons in this case, because from the excited singulet states usually pairs of oppositely charged solitons evolve, which attract each other, and thus would move anyway closer together also in reality. Thus such a pair of solitons would be much less affected by the length of the chains under consideration. Further, as expected, we obtain a complete bleaching of the band to band excitation.

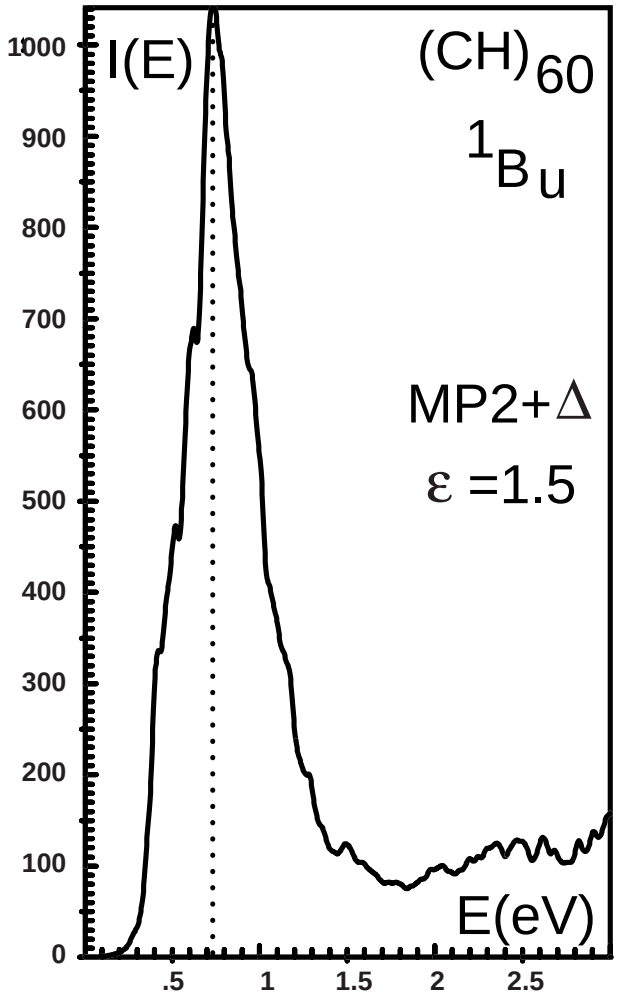

Figure 21 *Electronic spectrum of an even numbered chain of 60 units in the first excited singulet state (^1B_u), calculated as described in the text and in Appendix D in the supplementary material. The vertical line indicates the position of the soliton peak (charged solitons). The intensities I(E) are in arbitrary units (corresponding to the equations given in Appendix D in the supplementary material)*

Dynamics of cis-polacetylene (cPA) chains [70]

As mentioned already in the Introduction, in cPA we do not have a degenerate ground state. Since such a system cannot be described with a normal SSH model having the same resonance integrals and electron-phonon coupling strengths, we decided to perform a reparametrization of our PPP Hamiltonian for this system again. As in tPA we did that on the basis of correlated *ab initio* calculations on a small segment of cPA, namely cis-hexatriene. We found that in a model containing electron-electron interaction it is not necessary to introduce a symmetry breaking on the level of the one-particle parameters as it is suggested in the Brazowskii-Kirova model [71]. On the contrary, the symmetry breaking results almost exclusively from the two-electron interaction term, because there, the different geometrical arrangements in the two different bond alternation phases are naturally included via the Ohno approximation which makes the two-electron integrals geometry dependent. However, we found, that the resonance integrals have a value of -3.1 eV in cPA, by 0.6 eV larger in absolute value than in tPA, in order to match the dimerization energies of the system as given in the literature [72] and scaled for the inclusion of correlation. The symmetry breaking in the β parameter at alternating sites amounts only to 1.8% of the actual value quoted above. The energy difference between the two bond alternation phases is in our model

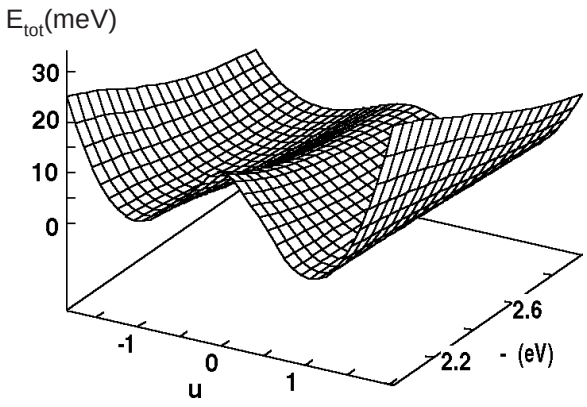

Figure 22 *The total potential energy E_{tot} per CH unit in a cPA chain of 9 CH units as a function of the bond alternation u (in Å) and the resonance integral β (the other parameters are determined such that the results of our ab initio calculations are well fitted by the model)*

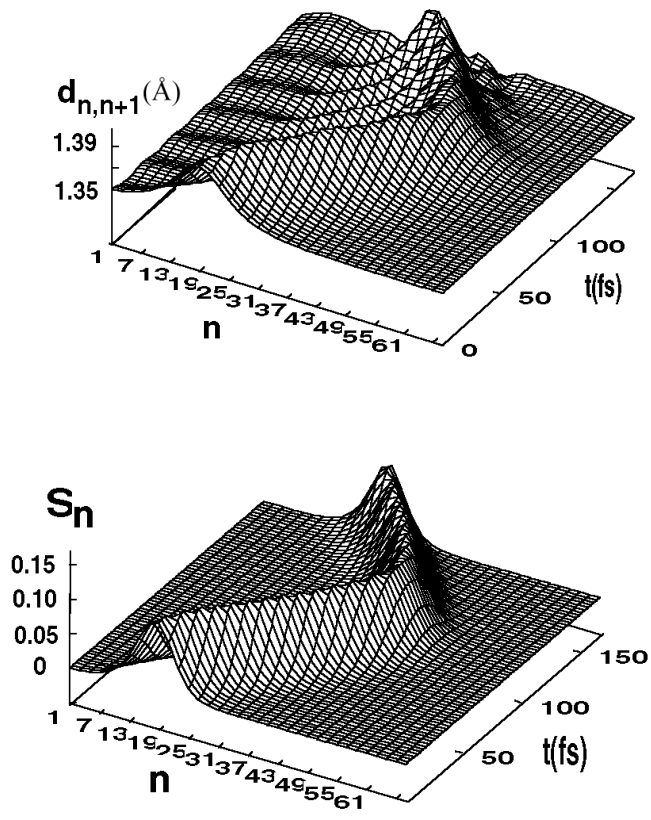

Figure 23 *Distance between two neighbouring sites $d_{n,n+1}$ and the spin densities at odd numbered sites S_n as functions of site and time in a cPA chain with 70 units, carrying one excess electron and an optimized polaron like distortion close to the chain end in the initial geometry*

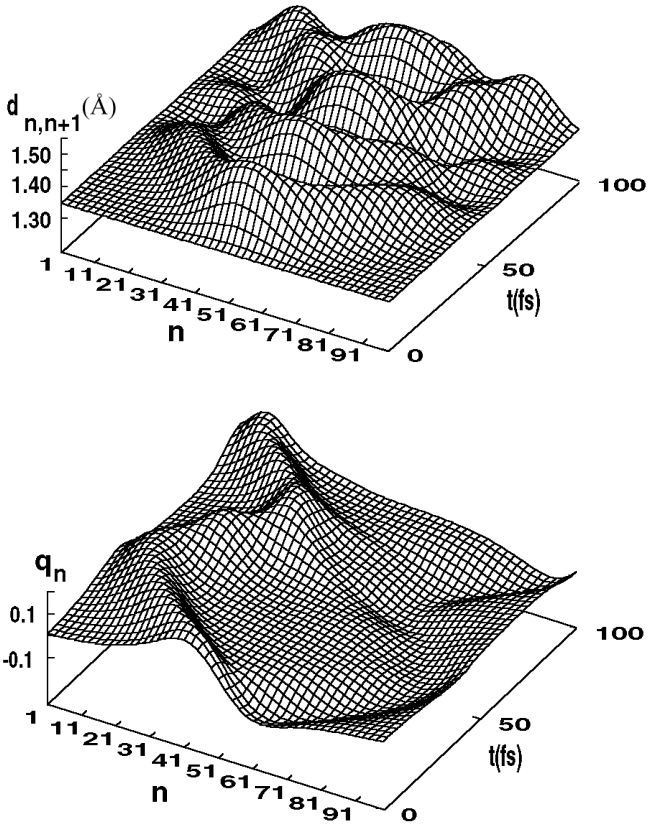

Figure 24 *Distance between two neighbouring sites $d_{n,n+1}$ and the charge densities at odd numbered sites q_n as functions of site and time in a cPA chain with 100 units in a pure A-phase geometry initially, carrying two excess electron*

smaller than the theoretical values quoted in the literature, however, these values differ significantly when calculated with different theoretical approximations [72,73]. Thus we did not bother to reproduce such values in our parametrization. The electron-phonon coupling strength we have determined as being 0.068 eV/Å with a symmetry breaking of only 3.7%. This value is comparable to the one in tPA (note, that the numerical value differs, because in both models the values refer to different definitions of the geometry). In Fig. 22 we show the total potential energy of an odd-numbered cPA chain as function of the bond alternation u and the resonance integral β [70]. However, in this parametrization the bipolaron width tends to increase with increasing chain length. Within the criteria for our parameters we were able to increase the symmetry breaking considerably bringing it closer to theoretical results given in the literature. With these sets of parameters the bipolaron width converges to a finite value with increasing chain length. Thus we are convinced that in cPA doubly charged bipolarons are stable with respect to the formation of a pair of singly charged polarons [70].

In our geometry optimizations we found that for singly charged chains polarons are the stable excitations, while for doubly charged chains we found bipolarons to be stable, which in turn serve as spinless charge carriers in this system instead of the solitons found in tPA. In Fig. 23 we show the dynamics of a longer cPA chain carrying one extra charge and with the optimized polaron geometry placed at one end of the chain in the initial geometry. The plot indicates clearly that polarons are just as mobile as solitons in tPA. The charge density follows closely the spin density S_n and therefore is not shown here. In the polaron we found [70] that as expected the nonlinear quasiparticle exhibits phase A geometry on both of its sides, while in its center there is no well established B-phase geometry, but rather a short segment with the equidistant geometry. To avoid the effects of spin contamination we have again used the AUHF approximation in our PPP calculations.

Note, that simulations on singly charged even numbered chains in a pure A-phase geometry also showed the formation of singly charged polarons. However, such a polaron would not be a spinless charge carrier, because besides a charge, it carries also a spin. Therefore we have studied the dynamics of doubly charged even numbered chains in A-phase

geometry initially. As Fig. 24 shows, a bipolaron is formed from that initial condition.

To show the fact that the formation of a bipolaron is favoured over that of two charged polarons, we have selected from the above simulation the times where the total potential energy exhibits maxima and minima, plotted the distances between neighbouring sites $d_{n,n+1}$ (at odd n only) at these times and compared it with the optimized bipolaron geometry in a chain of that length. Note, that in the bipolaron, in contrast to the polaron, a fully developed segment of B-phase geometry is formed. The result is shown in Fig. 25. The figure shows clearly, that the geometry at an energy minimum always corresponds best to the optimized bipolaron geometry, while at the energy maxima of that simulation always two charged polarons are formed. This indicates clearly, that in contrast to the results reported by Shimoi and Abe [74] obtained with the PPP-UHF method, a bipolaron is stable compared to the formation of two separated singly charged polarons. We assume, that the UHF method used by Shimoi and Abe [74] lead to different results due to spin contaminations inherent in that method.

SSH simulations on cPA [75] lead to results which are qualitatively similar to ours, however, a direct comparison is not possible, because in that case the difference between the energies of the two phases were far too large [75]. However, our PPP optimization results agree fairly well with those obtained with the Local Spin Density formalism [76]. Finally, the results on cPA indicate that our methodology does not only work well for solitons in tPA but also for polarons and bipolarons in cPA.

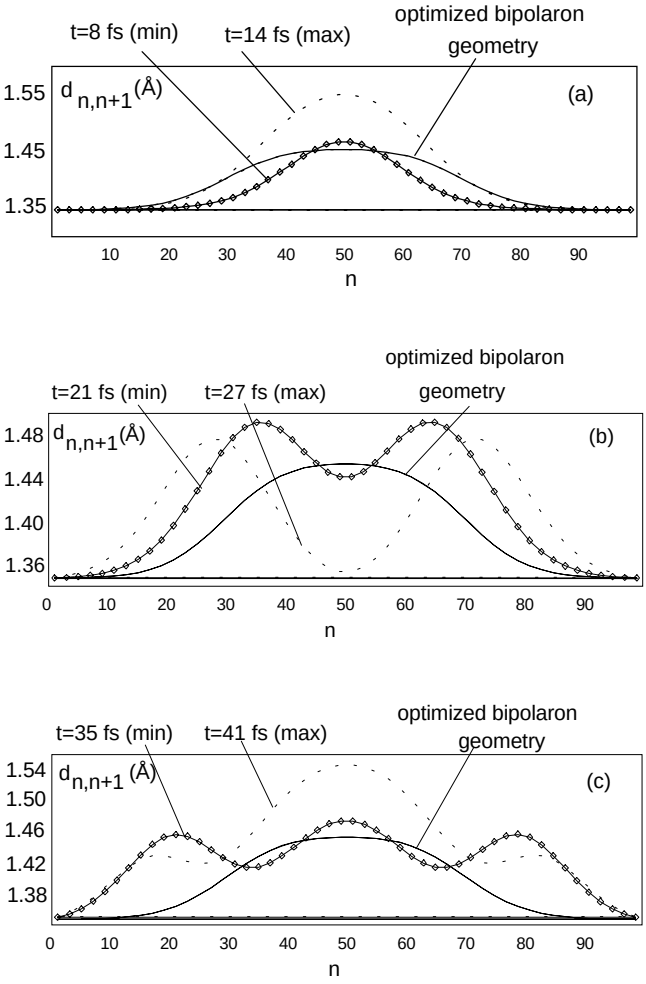

Figure 25 *The distances $d_{n,n+1}$ for even numbers n as function of site n from the simulation shown in the previous figure, at different times t which correspond to minima (min) and maxima (max) of the total potential energy together with the optimized bipolaron geometry in a chain of 100 units length*

Conclusions and outlook

To summarize, we have presented a simple and cheap model which

(i) yields a semi-quantitatively correct description of the dynamics of nonlinear charge carriers in conjugated polymers and of their spectra

(ii) can be applied to different systems by a simple reparametrization

(iii)allows also a quantum description of the dynamics.

The chemical stability of conducting polymers can be investigated with the help of correlated *ab initio* calculations on the infinite systems. The methods used for such calculations are documented completely in the literature (see ref. [52] for a comprehensive review and further references). Important for conducting polymers is their stability against oxygen. Thus one can calculate the interaction energies of the polymer with oxygen, by placing one oxygen molecule into each elementary cell in different orientations. Also properties like the bulk modulus and others can be computed by *ab initio* methods [52]. Single oxygen molecules interacting with an infinite chain can be studied with the help of Green's functions methods [52]. For these purposes also *ab initio* density functional (DFT) methods would be appropriate, since they yield results of MP2-quality for ground state properties already at the cost of a HF calculation, while the problems of DFT methods with excited states do not play a role here. Further, methods for the treatment of local perturbations in infinite chains can be implemented on DFT level also.

For the future we want to extend our simulations with the help of all valence electron semiempirical methods, like AM1, PM3 or others to be able to take into account also effects like the breaking of bonds. However, this can, in principle, also be done by using a Morse-type potential for the σ-electrons instead the harmonic one. The Carr-Parinello simulation method using density functional theory is computationally too costly for chains of our size. Further, we are convinced that our PPP model is already adequate to take most of the important effects into account. Calculations with better methods are planned only for comparisons and testing purposes. All together, a combination of calculations such as

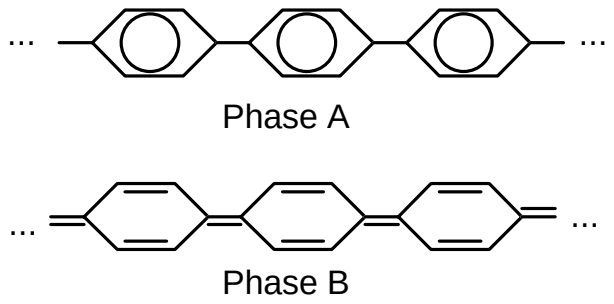

Figure 26 *Sketch of two different bond alternation phases A (aromatic) and B (quinoidal) in polyparaphenylene*

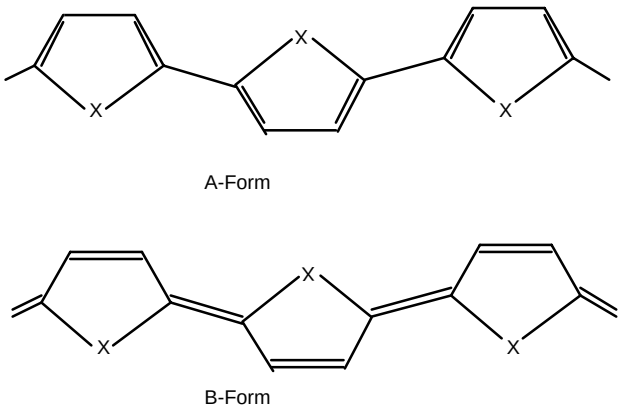

Figure 27 *Sketch of the two different bond alternation phases A (aromatic) and B (quinoidal) in the polythiophene type polymers (X=O, N or S)*

(i) the present model which yields information on existence, structure and mobility (including temperature effects, electric fields and neighbouring chains) of nonlinear quasiparticles and

(ii) correlated *ab initio* crystal orbital methods which yield informations on the chemical stability of a polymer and its mechanical properties,

should be a reliable tool for the theoretical prediction of useful chemical structures which can be used as synthetic metals.

Other conjugated polymers, where nonlinear charge carriers can appear are too numerous to list them all here. We will just mention some of them where we also plan to test our method on. Mostly they do not exhibit degenerate ground states, but bond alternation phases with slightly different energies. Thus in these systems solitons would be unstable, because on one side of the soliton the energetically unfavourable alternation phase would exist. An example is polyparaphenylene, where we have an energetically low-lying aromatic phase A and a higher lying quinoidal phase B as sketched in Figure 26. However, here as in cPA polarons would be stable, because dependent on the width of the polaron the length of the B-segment could be kept small: $(A)_n$-$(B)_{n'}$-$(A)_m$. Spinless charge carriers in the system would then be bipolarons, i.e., doubly charged polarons.

To apply our procedure to this system, we have to define a coordinate which switches from the A-phase with aromatic rings and long bonds between them, via the equidistant one, where all bonds have equal length to the B-form with quinoidal structure having short bonds between the quinoidal rings. Then on a small model system like bi- or triphenyl we can optimize the two structures to fix the geometry on the basis of high quality correlated *ab initio* or density functional calculations. Then we can calculate again on *ab initio* level the potential curve with respect to this generalized coordinate and parametrize the PPP-Hamiltonian such that it is able to reproduce this potential curve. Then the PPP Hamiltonian can be used to perform dynamic simulations on long chains and to study the mobility and stability of the carriers at finite temperatures. Further, one can compute their spectra in the gap. Another interesting feature of this system is, that the rings are rotated against each other and thus electron-libron coupling can also contribute to the nonlinear effects. *Ab initio* calculations on the polymer and its derivates have been published [39,46,47,49,77].

Other systems with two non-degenerate minimum structures are polyfurane (X=O), polythiophene (X=S) and polypyrrole (X=N), polymers which are known to become conducting upon doping. Here we have again an aromatic A- and a quinoidal B-form (Figure 27). *Ab initio* studies on the infinite polymers and their derivates have been performed by Bhakshi *et al.* [51]. However, in these cases even the exact nature of the charge carriers is still under discussion. Thus our method, including a reparametrization of the PPP Hamiltonian could be of help to settle the issue. *Ab initio* calculations would have to be performed again on a subunit, preferably a trimer of each species.

A very interesting system is the polyaniline with its different oxidation states, which can partly form similar structures as described above. One of its states, pernigraniline can also form solitons, because it has a degenerate ground state. Here again electron-libron couplings can become important as a contribution to the nonlinear effects. Such rotations between rings can be incorporated by representing the hopping integrals as a function of the rotation angles, most probably a cosine function, in addition to the usual electron-phonon coupling. Further one would have to incorporate an additional term in the σ-electron potential, which describes the sterical hindrance as function of the rotation angle. Such a term should have the form,

$$V_{HH} = \frac{K_{HH}}{2} \sum_j \sin^2\left[\vartheta_{j,j+1} - (-1)^j \vartheta_0\right] \qquad (3)$$

Here $\vartheta_{j,j+1}$ is the displacement of the rotation angle between sites j and j+1, and ϑ_0 is the angle in the undistorted structure. The hopping integrals for the bonds between rings are modulated by a factor $\cos(\vartheta_{j,j+1})$. The same reasoning holds for polyparaphenylene. The chemical structures of two oxi-

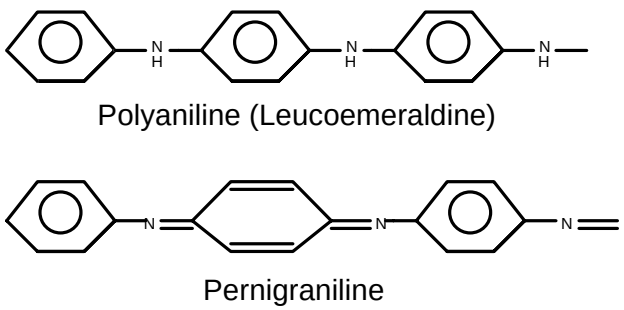

Figure 28 *Two different oxidation states of the polyaniline system*

dation states of the system which exhibit nonlinear charge carriers are shown in Figure 28.

Polaron structures have also been reported for fullerenes. They have been found in SSH type model calculations. The fullerenes show dimerization, while in the string-polarons formed upon excitations or doping the dimerization is removed along an equatorial circle which can rotate around the center of the fullerene. However, in this case the parameters appropriate for tPA could be used. The hopping part of the Hamiltonian would have SSH from:

$$\hat{H}^{Res} = \sum_{\langle ij \rangle} \sum_{\sigma} \left[\beta_0 + \alpha \left(u_i^{(j)} + u_j^{(i)} \right) \right] \left(\hat{c}_{i\sigma}^{+} \hat{c}_{j\sigma} + \hat{c}_{j\sigma}^{+} \hat{c}_{i\sigma} \right) \tag{4}$$

where the sum denotes summation over all covalently bound ij-pairs. $u_i^{(j)}$ denotes a displacement of unit i into the direction of unit j [78-80]. The rest of the PPP Hamiltonian would be the same as that discussed for tPA, only now the γ's have to be computed from the three dimensional structure of the fullerene ball. The σ-potential has the form,

$$V^{\sigma} = \frac{K}{2} \sum_{\langle ij \rangle} \left(a + u_i^{(j)} + u_j^{(i)} - R_0 \right)^2 + V^{rad} \tag{5}$$

where a is the bond distance in the equidistant system and R_0 again the equilibrium CC-σ bond distance. V^{rad} contains force constants according to changes in bond angles, where the angles denote displacements from the ideal bond angles:

$$V^{rad} = \sum_i \left\{ \frac{K_1}{2} \left(108° - \vartheta_i^{(1)} \right)^2 + \frac{K_2}{2} \left[\left(120° - \vartheta_i^{(2)} \right)^2 + \left(120° - \vartheta_i^{(3)} \right)^2 \right] \right\} \tag{6}$$

Each carbon i belongs to a pentagon and two fused hexagons. The angles used above are the bond angles around this carbon atom i, where $\vartheta_i^{(1)}$ is in the pentagon, and the other two are the angles in the two hexagons. Studies on all these systems are in progress in our laboratory.

Acknowledgement Major parts of the derivations given in Appendix A in the supplementary material for the results presented in Section III of this work have been completed during a stay of one of us (W.F.) at the „Center for Theoretical Studies of Physical Systems“ at Clark Atlanta University, Atlanta, Georgia, USA in April, 1996. W.F. wants to thank all members of the Center for their kind hospitality, especially Professors C. Handy and A. Z. Msezane who also made his stay at the Center possible.

References

1. (a) Su, W. P.; Schrieffer, J. R.; Heeger, A. J. *Phys. Rev. Lett.* **1979**, *42*, 1698. (b) Su, W. P. *Solid State Commun.* **1980**, *35*, 899. (c) Su, W. P.; Schrieffer, J. R.; Heeger, A. J. *Phys. Rev.* **1980**, *B22*, 2099. (d) Heeger, A. J.; Kivelson S.; Schrieffer J. R.; Su W. P. *Rev. Mod. Phys.* **1988**, *60*, 781. (e) Förner, W. *J. Mol. Model.* **1996**, *2*, 70. (f) Förner, W. *J. Mol. Model.* **1996**, *2*, 103. (g) Förner, W. *J. Mol. Model.* **1997**, *3*, 78.
2. (a) Thomann, H.; Dalton, L. R.; Tomkiewicz, Y.; Shiren, N. S.; Clarke, T. C. *Phys. Rev. Lett.* **1983**, *50*, 533. (b) Thomson, H.; Kim, H.; Morrobel-Sosa, A.; Dalton, L. R.; Jones, M. T.; Robinson, B. H.; Clarke, T. C.; Tomkiewicz, Y. *Synth. Met.* **1984**, *9*, 255. (c) Thomann, H.; Cline, J. E.; Hofmann, B. M.; Kim, H.; Morrobel-Sosa, A.; Robinson, B. H.; Dalton, L. R. *J. Phys. Chem.* **1985**, *89*, 1994. (d) Heeger, A. J.; Schrieffer, J. R. *Solid State Commun.* **1983**, *48*, 207. (e) Soos, Z. G.; Ramashesha, S. *Phys. Rev. Lett.* **1983**, *51*, 2374.
3. Sasai, M.; Fukutome, H. *Synth. Met.* **1984**, *9*, 295.
4. (a) Orenstein, J.; Baker, G. L. *Phys. Rev. Lett.* **1982**, *49*, 1043. (b) Weinberger, B. R. *Phys. Rev. Lett.* **1983**, *50*, 1693. (c) Blanchet, G. B.; Fincher, C. P.; Heeger, A. J. *Phys. Rev. Lett.* **1983**, *51*, 2132. (d) Blanchet, G. B.; Fincher, C. P.; Chung, T. C.; Heeger, A. J. *Phys. Rev. Lett.* **1983**, *50*, 1938.
5. Bishop, A. R.; Campbell, D. K.; Lomdahl, P. S.; Horovitz, B.; Phillpot, S. R. *Phys. Rev. Lett.* **1984**, *52*, 671.
6. Wang, C. L.; Martino, F. *Phys. Rev.* **1986**, *B34*, 5540.
7. (a) Su, W. P. *Phys. Rev.* **1986**, *B34*, 2988. (b) Kivelson, S.; Wu, W.-K. *Phys. Rev.* **1986**, *B34*, 5423.
8. Förner, W. *Chem. Phys.* **1992**, *160*, 173.
9. Su, W. P.; Schrieffer, J. R. *Proc. Natl. Acad. Sci. USA* **1980**, *77*, 5626.
10. Förner, W.; Seel, M.; Ladik, J. *Solid State Commun.6* **1986**, *57*, 463.
11. Förner, W.; Seel, M.; Ladik, J. *J. Chem. Phys.* **1986**, *84*, 5910.
12. (a) Liegener, C.-M.; Förner, W.; Ladik, J. *Solid State Commun.* **1987**, *61*, 203. (b) Godzik, A.; Seel, M.; Förner, W.; Ladik, J. *Solid State Commun.* **1986**, *60*, 609. (c) Orendi, H.; Förner, W.; Ladik, J. *Chem. Phys. Lett.* **1988**, *150*, 113.
13. Förner, W. *Solid State Commun.* **1987**, *63*, 941.

14. Gibson, H. W.; Weagley, R. J.; Mosher, R. A.; Kaplan, S.; Prest, W. M.; Epstein, A. J. *Phys. Rev.* **1985**, *B31*, 2338.
15. Förner, W.; Wang, C.-L.; Martino, F.; Ladik, J. *Phys. Rev.* **1988**, *B37*, 4567.
16. Boudreaux, D. S.; Chance, R. R.; Bredas, J. L.; Silbey, R. *Phys. Rev.* **1983**, *B28*, 6927.
17. Phillpot, S. R.; Baeriswyl, D.; Bishop, A. R.; Lomdahl, P. S. *Phys. Rev.* **1987**, *B35*, 7533.
18. Markus, R.; Förner, W.; Ladik, J. *Solid State Commun.* **1988**, *68*, 1.
19. Förner, W. *Phys. Rev.* **1991**, *B44*, 11743.
20. Förner, W. *Chem. Phys.* **1992**, *160*, 188.
21. Nakahara, M.; Maki, K. *Phys. Rev.* **1982**, *B25*, 7789.
22. Rukh, R.; Sigmund, E.; Eisele, H. *J. Chem. Phys.* **1989**, *90*, 6463.
23. (a) Davydov, A. S.; Kislukha, N. I. *Phys. Stat. Sol.* **1973**, *B59*, 465. (b) Davydov, A. S. *Phys. Scripta* **1979**, *20*, 387.
24. (a) Davydov, A. S. *Zh. Eksp. Teor. Fiz.* **1980**, *78*, 789. (b) *Sov. Phys. JETP* **1980**, *51*, 397.
25. (a) Förner, W. *Habilitation Thesis*, University Erlangen-Nürnberg, FRG **1992**. (b) *J. Phys.: Cond. Matter* **1994**, *6*, 9089.
26. Förner, W. *J. Phys.: Cond. Matter* **1993**, *5*, 803.
27. Skrinjar, M. J.; Kapor, D. V.; Stojanovic, S. D. *Phys. Rev.* **1988**, *A38*, 6402.
28. Mechtly, B.; Shaw, P. B. *Phys. Rev.* **1988**, *B38*, 3075.
29. Förner, W. *J. Phys.: Cond. Matter* **1992**, *4*, 1915.
30. Förner, W. *J. Phys.: Cond. Matter* **1993**, *5*, 3883.
31. (a) Motschmann, H.; Förner, W.; Ladik, J. *J. Phys.: Cond. Matter* **1989**, *1*, 5083. (b) Förner, W.; Ladik, J. In *Davydov's soliton revisited*; Christiansen, P. L.; Scott, A. C., Eds.; Plenum: New York, 1990; p 267.
32. (a) Förner, W. *J. Phys.: Cond. Matter* **1991**, *3*, 4333. (b) *J. Comput. Chem.* **1992**, *13*, 275. (c) *Nanobiology* **1992**, *1*, 413.
33. (a) Davydov, A. S. *Teor. Mat. Fiz.* **1979**, *40*, 408. (b) *Phys. Stat. Sol.* **1988**, *B146*, 619. (c) *Nonlinearity* **1989**, *2*, 383.
34. Abramowitz, A.; Stegun, I. A. *Handbook of mathematical functions*, 9th ed.; Dover: New York, 1970, pp 896 - 897.
35. Förner, W. *Synth. Met.* **1989**, *30*, 135.
36. (a) Förner, W. *Adv. Quantum Chem.* **1994**, *25*, 207. (b) *Ind. J. Chem. Section (A)* **1997**, *36A*, 355-392.
37. Schinke, R.; Engel, V. *J. Chem. Phys.* **1990**, *93*, 3252.
38. Majewski, J. A.; Vogl, P. *Phys. Rev.* **1992**, *B46*, 12219,12235.
39. Ambrosch-Draxl, C.; Majewski, J. A.; Vogl, P.; Leising, G. *Phys. Rev.* **1995**, *B51*, 9668.
40. Slater, J. C. *Quantum theory of molecules and solids*; McGraw-Hill: New York, 1974, Vol. 4.
41. Becke, A. D. *Phys. Rev.* **1988**, *A38*, 3098.
42. Becke, A. D. *J. Chem. Phys.* **1993**, *98*, 5648.
43. Vosko, S. H.; Wilk, L.; Nusair, M. *Can. J. Phys.* **1980**, *58*, 1200.
44. Lee, C.; Yang, W.; Parr, R. G. *Phys. Rev.* **1988**, *B37*, 785.
45. Perdew, J. P.; Wang, Y. *Phys. Rev.* **1986**, *B33*, 8800.
46. Bakhshi, A. K.; Ladik, J. *Ind. J. Chem.* **1994**, *13*, 494.
47. Bakhshi, A. K. *Superlattices and Microstructures* **1992**, *11*, 465.
48. Bakhshi, A. K. *Ann. Rep. Roy. Soc. Chem.* **1992**, *C89*, 147.
49. Bakhshi, A. K.; Ladik, J. *Synth. Met.* **1989**, *30*, 115.
50. Bakhshi, A. K.; Yamaguchi, Y.; Ago, H.; Yamabe, T. *Synth. Met.* (in press).
51. Bakhshi, A. K.; Ago, H.; Yoshizawa, K.; Tanaka, K.; Yamabe, T. *J. Chem. Phys.* **1996**, *104*, 5528.
52. Ladik, J. *Quantum theory of polymers as solids*; Plenum: New York, London, 1988.
53. König, G.; Stollhoff, G. *Phys. Rev. Lett.* **1990**, *65*, 1239.
54. (a) Suhai, S. *Phys. Rev.* **1994**, *B50*, 14791. (b) **1995**, *B51*, 16553.
55. (a) Villar, H. O.; Dupuis, M.; Watts, J. D.; Hurst, G. J. B.; Clementi, E. *J. Chem. Phys.* **1988**, *88*, 1003. (b) Villar, H. O.; Dupuis, M.; Clementi, E. *J. Chem. Phys.* **1988**, *88*, 5252. (c) *Phys. Rev.* **1988**, *B37*, 2520.
56. Amos, T.; Snyder, L. C. *J. Chem. Phys.* **1964**, *41*, 1773.
57. (a) Martino, F.; Ladik, J. *J. Chem. Phys.* **1970**, *52*, 2262. (b) *Phys. Rev.* **1971**, *A3*, 862. (c) Mayer, I.; Ladik, J.; Biczo, G. *Int. J. Quantum Chem.* **1973**, *7*, 583. (d) Rosenberg, M.; Martino, F. *J. Chem. Phys.* **1975**, *63*, 5354.
58. Kovar, T. *Master's Thesis*, University Erlangen-Nürnberg **1986**.
59. (a) Förner, W. *Phys. Rev.* **1991**, *B44*, 11743. (b) *J. Mol. Struct. (Theochem)* **1993**, *282*, 235.
60. Soos, Z. G.; Ramashesha, S. *Phys. Rev. Lett.* **1983**, *51*, 2374.
61. Suhai, S. *Habilitation Thesis*, Friedrich-Alexander-Univ. Erlangen-Nürnberg **1983**.
62. Suhai, S. *Phys. Rev.* **1983**, *B27*, 3506.
63. Suhai, S. *Phys. Rev.* **1984**, *B29*, 4570.
64. Suhai, S. *Int. J. Quant. Chem.* **1984**, *QBS11*, 223.
65. (a) Mehring, M.; Grupp, A.; Höfer, P.; Käss, A. *Synth. Met.* **1989**, *28*, D399. (b) Käss, H.; Höfer, P.; Grupp, A.; Kathol, P.; Wegner, G.; Mehring, M. *Europhys. Lett.* **1987**, *4*, 947.
66. Rubner, O.; Förner, W.; Ladik, J. *Synth. Met.* **1993**, *61*, 279.
67. Förner, W. *Ind. J. Chem.* **1994**, *33A*, 461.
68. Block, S.; Streitwolf, H. W. *Synth. Met.* **1996**, *76*, 31.
69. Feldblum, A.; Kaufman, J. H.; Etemad, S.; Heeger, A. J.; Chung, T.-C.; McDiarmid, A. G. *Phys. Rev.* **1982**, *B26*, 815.
70. Utz, W.; Förner, W. *Phys. Rev. B* (accepted).
71. Brazowskii, S.; Kirowa, N. *JETP. Lett* **1981**, *33*, 4.
72. (a) Suhai, S. *J. Chem. Phys.* **1980**, *73*, 3843. (b) Suhai, S. *Phys. Rev.* **1995**, *B51*, 16533.
73. (a) Dovesi, R. *Intern. J. Quantum Chem.* **1984**, *26*, 197. (b) Karpfen, A.; Höller, R. *Solid State Commun.* **1981**, *37*, 179.
74. Shimoi, Y.; Abe, S. *Synth. Met.* **1995**, *69*, 687.
75. Wang, C.; Su, Z.; Martino, F. *Phys. Rev.* **1986**, *B33*, 1512.
76. Ye, L.; Freeman, A.; Ellis, D.; Delley, B. *Phys. Rev.* **1989**, *B40*, 6285.

77. Bogar, F.; Förner, W.; Kapuy, E.; Ladik, J. *J. Mol. Struct. (Theochem)* **1997**, *391*, 193.
78. Friedman, B. *Phys. Rev.* **1992**, *B45*, 1454.
79. Harigaya, K. *Phys. Rev.* **1992**, *B45*, 13676.
80. You, W. M.; Wang, C. L.; Su, Z. B. *Phys. Rev.* **1993**, *B47*, 4765.
81. Cruzeiro-Hansson, L.; Okhonin, V. A.; Khlebopros, R. G.; Yassievich, I. N. *Nanobiology* **1992**, *1*, 395.
82. Cruzeiro-Hansson, L. *Phys. Rev. Lett.* **1994**, *73*, 2927.
83. Förner, W. *J. Phys.: Cond. Matter*, submitted.
84. Heller, E. J. *J. Chem. Phys.* **1978**, *48*, 2067.
85. Fincher, Jr. C. R.; Chen, C. E.; Heeger, A. J.; MacDiarmid, A. G.; Hastings, J. B. *Phys. Rev. Lett.* **1982**, *48*, 100.
86. Vogl, P.; Campbell, D. K. *Phys. Rev.* **1990**, *41*, 12797.
87. Ohno, K. *Theor. Chim. Acta* **1964**, *2*, 219.
88. Amos, T.; Hall, G. G. *Proc. Roy. Soc. (London)* **1961**, *A263*, 483.
88. Suhai, S.; Ladik, J. *J. Phys.* **1982**, *C15*, 4327.
90. (a) Suhai, S. *Phys. Rev.* **1984**, *B29*, 4570. (b) *Int. J. Quant. Chem.* **1984**, *QCS11*, 223. (c) *J. Mol. Struct. (Theochem)* **1985**, *123*, 97. (d) *Int. J. Quan. Chem.* **1986**, *29*, 469.
91. Liegener, C.-M. *J. Phys.* **1985**, *C18*, 6011.
92. Liegener, C.-M.; Ladik, J. *Phys. Rev.* **1987**, *B35*, 6403.
93. Förner, W. *Phys. Scripta*, submitted.